

AEDC-TR-72-42

APR 13 1972

APR 26 1972

FEB 18 1976

cy 2



EXPERIMENTS ON THE STARTING PROCESS IN A LUDWIG TUBE

Dominic J. Cagliostro
Yale University

March 1972

Approved for public release; distribution unlimited.

**ARNOLD ENGINEERING DEVELOPMENT CENTER
AIR FORCE SYSTEMS COMMAND
ARNOLD AIR FORCE STATION, TENNESSEE**

PROPERTY OF U S A
AEDC LIBRARY
F40600-72-C-0003

NOTICES

When U. S. Government drawings specifications, or other data are used for any purpose other than a definitely related Government procurement operation, the Government thereby incurs no responsibility nor any obligation whatsoever, and the fact that the Government may have formulated, furnished, or in any way supplied the said drawings, specifications, or other data, is not to be regarded by implication or otherwise, or in any manner licensing the holder or any other person or corporation, or conveying any rights or permission to manufacture, use, or sell any patented invention that may in any way be related thereto.

Qualified users may obtain copies of this report from the Defense Documentation Center.

References to named commercial products in this report are not to be considered in any sense as an endorsement of the product by the United States Air Force or the Government.

EXPERIMENTS ON THE STARTING
PROCESS IN A LUDWIEG TUBE

Dominic J. Cagliostro
Yale University

Approved for public release; distribution unlimited.

FOREWORD

The work reported herein was sponsored by Headquarters, Arnold Engineering Development Center (AEDC), Air Force Systems Command (AFSC), Arnold Air Force Station, Tennessee, under Program Element 65802F. Technical monitoring of the contract was performed by Captain Carlos Tirres, USAF, Research and Development Division, Directorate of Technology.

The effort was conducted from June 1970 to January 1972 at Yale University under Contract F40600-70-C-0008. The manuscript was submitted for publication in January 1972.

The author is indebted to the principal investigator, Professor Peter P. Wegener, and to Dr. Leo T. Smith for assistance, many helpful discussions, and parts of this report. The advice of Professor E. Becker and Dr. E. Piltz, both at the Institute of Mechanics, Technische Hochschule, Darmstadt, Germany is gratefully acknowledged. The uniform flow nozzles used here were designed by Mr. Robert L. P. Voisinet of the U. S. Naval Ordnance Laboratory. Further thanks is extended to the U. S. Naval Ordnance Laboratory for loaning us the Zeiss Mach-Zehnder interferometer which was utilized in many of the experiments.

The reproducibles used in the reproduction of this report were supplied by the author.

This technical report has been reviewed and is approved.

Carlos Tirres
Captain, USAF
Research & Development
Division
Directorate of Technology

Robert O. Dietz
Acting Director
Directorate of Technology

ABSTRACT

An experimental investigation of the starting process in the Ludwig tube, an intermittent type tube wind-tunnel, was conducted with emphasis on the effects of nozzle-test section geometry. In particular the semi-open and closed jet configuration was studied. Dry air at 1.0 and 2.0 atm pressure and room temperature was used in the supply tube and a quick opening diaphragm located downstream of the nozzle and test section was employed to initiate the flow. Spark shadowgraph pictures, high-speed shadowgraph movies, streak interferograms, and pressure measurements were made in $M = 1.67$ and 3.0 continuously expanding nozzles and $M = 1.6$ and 2.5 parallel flow nozzles. Results show that the nozzle-test section geometry significantly affects the starting process in the $M = 1.60$ and 1.67 nozzles. In the semi-open jet configuration supersonic flow was established without the formation of starting shocks, while in the closed jet configuration a starting shock wave did occur. Boundary layer thickening and flow separation occurred during the starting process in the $M = 2.50$ and 3.0 nozzles. Adverse pressure and density gradients were measured in the nozzle during the starting process. This effect appears to cause the observed boundary layer thickening and flow separation which occur during that period in the $M = 2.5$ and 3.0 nozzles. These results indicate that viscous effects are important during the starting process in a Ludwig tube under the conditions tested here. It was found that the presence of a model in the $M = 1.67$ nozzle in a closed jet configuration increased the starting times.

CONTENTS

	<u>Page</u>
ABSTRACT	iii
NOMENCLATURE	ix
I. INTRODUCTION	1
II. EXPERIMENTAL APPARATUS	7
III. EXPERIMENTAL RESULTS	9
IV. DISCUSSION OF RESULTS	26
V. SUMMARY	29
APPENDIX: DETAILED DESCRIPTION OF LUDWIG TUBE WIND TUNNEL NOZZLES AND AUXILIARY EQUIPMENT	31
REFERENCES	41

ILLUSTRATIONS

Page

- Figure 1 Ludwig Tube: Simplified $t - x$ plot. The times schematically indicated are t_i , the total starting time; t_{i1} , the time required to establish sonic conditions at the nozzle's throat; t_m , the total time of steady supersonic flow. 2
- Figure 2 Experimental Apparatus. (A) High Speed Camera. (B) Pressure Transducer (at upstream position). (C) Mach-Zehnder Interferometer. (D) Side View of Test Section. Supply tube: 5.30 in. I.D. Dump tube: 3.76 in. I.D. Nozzle: 2" x 2" at throat ($M = 1.67$ at exit). (E) Collimating Lens and Light Source. (F) Oscilloscope to record pressure traces. 6
- Figure 3 Shadowgraph High-Speed Movie Prints of Starting Process in the Y160 Nozzle, (A) Semi-Open Jet, (B) Closed Jet, (C) Semi-Open Jet with a Wedge Model at Nozzle Exit. The time between each frame is about 0.22 msec; field of view shows nozzle throat at left and three inches downstream. Flow is from left to right. 10
- Figure 4 Streak Interferograms of Starting Process in the Y160 Nozzle, (A) Semi-Open Jet and (B) Closed Jet. The t and x axes are shown; field of view is nozzle throat at left and three inches downstream. Decreasing densities are indicated by the motion of fringes from left to right. 12
- Figure 5 Density Measurements in Y160 Nozzle, (A) Semi-Open Jet and (B) Closed Jet Configuration. The density along 2.0 inches of the nozzle centerline starting at the nozzle throat, $x = 0.0$ " is shown for various times during the starting stage. 14

- Figure 6 Spark Shadowgraph Pictures of the Starting Process in the Y167 Nozzle, (A) Semi-Open Jet, and (B) Closed Jet Configuration. Field of view is 3.6 inches in flow direction, i.e., from left to right, with the nozzle exit at the center. Times are measured from diaphragm rupture time which is at $t = 0.0$. 15
- Figure 7 Spark Shadowgraph Pictures of the Starting Process in the Y167 Nozzle with a Wedge Model at Nozzle Exit, (A) Semi-Open Jet, and (B) Closed Jet Configuration. Field of view is 3.6 inches in flow direction, i.e., from left to right, with the nozzle exit at the center. Times are measured from diaphragm rupture time which is at $t = 0.0$. 16
- Figure 8 Shadowgraph High-Speed Movie Prints of Starting Process in the Y250 Nozzle, (A) Semi-Open Jet, (B) Closed Jet, (C) Semi-Open Jet with Model, and (D) Closed Jet with Model. The time between each frame is about 0.22 msec; field of view is 3.0 inches in flow direction, i.e., from left to right with the nozzle exit at the center. 18
- Figure 9 Spark Shadowgraph Pictures of the Starting Process in the Y300 Nozzle with a Wedge Model at Nozzle Exit, (A) Semi-Open Jet, and (B) Closed Jet Configuration. Field of view is 3.6 inches in flow direction, i.e., from left to right, with the nozzle exit at the center. Times are measured from diaphragm rupture time which is at $t = 0.0$. 20
- Figure 10 Pressure Measurements in the Y167 Nozzle, (A) Semi-Open Jet, and (B) Closed Jet Configuration. Positions are measured from nozzle throat in downstream direction; $P_4 = 1.0$ atm. Pressure trace is triggered at diaphragm rupture. 21

Figure 11 Pressure Measurements in the Y300 Nozzle, (A) Semi-Open Jet, and (B) Closed Jet Configuration. Positions are measured from nozzle throat in the downstream direction; $P_4 = 1.0$ atm. Pressure trace is triggered at diaphragm rupture. 22

Figure 12 Density Measurements in the Y160 Nozzle in the (A) Semi-Open Jet and (B) Closed Jet Configuration. Positions are measured from the nozzle throat in the downstream direction; $P_4 = 2.0$ atm. Time starts when initial expansion fan reaches a position 3.6 in. downstream from nozzle throat. 24

Table 1. Starting Times for the Y167 and Y300 Nozzles in the Semi-Open Jet and Closed Jet Configurations. Times were measured from the pressure traces made at positions along the nozzle centerline. The positions are measured from nozzle throat in the downstream direction. Times start when expansion fan reaches pressure transducer. Gas: Dry Air. Initial pressure: $P_4 = 1.0$ atm. 25

NOMENCLATURE

A	area
M	Mach number
P	pressure (atm)
R	radius of curvature
Re	Reynolds number
T	Temperature ($^{\circ}$ K)
t	time (msec)
t_i	total starting time
t_{i1}	time to establish sonic flow in nozzle throat
t_T	total time of steady supersonic flow
X	distance coordinate (in.)
ρ	density (g/cm^3)

SUBSCRIPTS

l	initial conditions in low pressure tube
4	initial conditions in high pressure tube
st	steady state

SUPERSCRIPTS

*	indicates property at the nozzle throat
---	---

I

INTRODUCTION

Wind tunnel testing plays an essential role in finding solutions to many problems in gas dynamics since exact analytical solutions have been obtained only for very restricted or simplified cases. For certain problems numerical methods prove to be applicable and desirable. However, this is not the case when the flow patterns are complicated and unstable, as in the case of flows with turbulent boundary layers, separation, vortex shedding, etc. For those flow fields, wind tunnel testing is necessary for obtaining needed design information. The significant conditions necessary for producing a similar flow field over a geometrically similar model in a wind tunnel are determined by the methods of dimensional analysis and similitude, e.g., Ref. 1 and 2. The resulting similarity parameters may be non-dimensional ratios of forces, energy fluxes, or other dimensionless groups of variables. For model testing of aircraft, missiles and launch vehicles, which fly at transonic or supersonic velocities at altitudes sufficiently low so that continuum theory holds, two significant similarity parameters, which must be duplicated in the test section, are the Mach number, M , and the Reynolds number, Re . The Mach number accounts for the compressibility effects of the gas, and the Reynolds number is a measure of the relative importance of inertial and viscous forces. If these parameters in the test section are the same as those for the flight conditions, predictions of drag and lift coefficients, boundary layer behavior of the prototype, etc., can be made based on experimental data from geometrically similar models.

Up to the present time, simulation of flight Mach numbers has usually been achieved, but Reynolds number simulation has not kept up with present and future Reynolds number requirements (e.g., Ref. 3). To simulate flight conditions of present day aircraft which fly at $M = 3$ at an altitude of 64,000 ft, the required Re would be about 2.2×10^8 , based on tunnel diameter*, however, for the same aircraft at $M = 1.5$ at an altitude of 45,000 ft, the required Re would be about 5.2×10^8 . Available facilities can only produce Reynolds numbers up to about 1.5×10^8 at this Mach number (Ref. 4). Future aircraft model testing will require an increase in the Re capabilities of at least an order of magnitude (e.g., Ref. 3 and 4). This increase must be

* Reynolds numbers here are based on the minimum tunnel diameter for noninterference of a Mach line from the model nose with the remainder of the configuration. (Ref. 4).

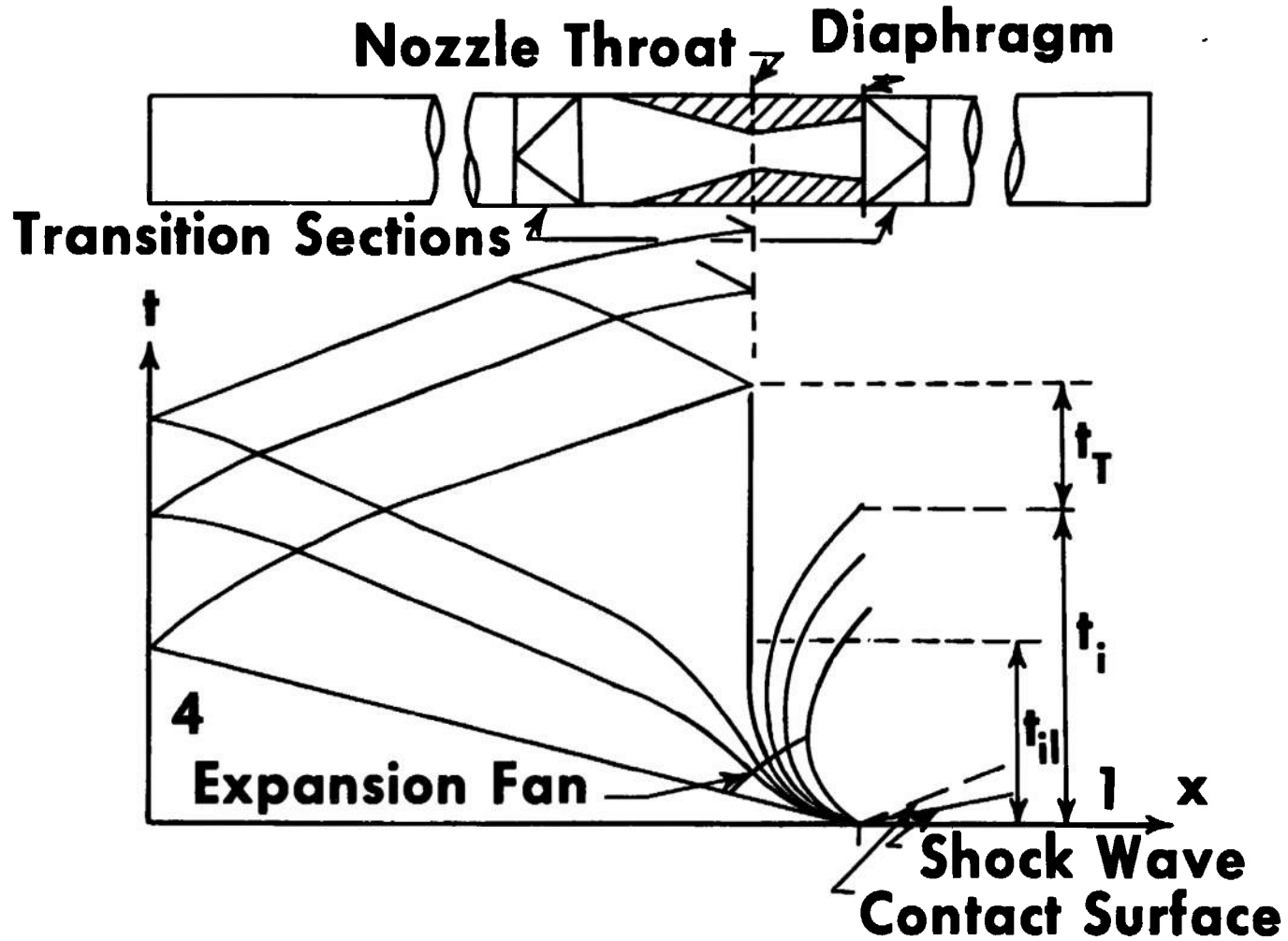


Fig. 1 Ludwieg Tube: Simplified $t-x$ plot. The times schematically indicated are t_i , the total starting time; t_{ii} , the time required to establish sonic conditions at the nozzle's throat; t_T , the total time of steady supersonic flow.

achieved if reliable data are to be obtained from wind tunnel testing. The most direct way to reach this goal is to increase the stagnation pressure of the gas in the test section, since Re is a linear function of stagnation pressure for air at moderate pressures and temperatures (Ref. 3). The maximum stagnation pressures that can be used in a facility are usually limited by the stress of the wind tunnel walls or of the model and sting support. Therefore, the model stress and tunnel wall stress (for a cylindrical shell) are linear functions of the Re number (or stagnation pressure), as shown by Fila (3). Technological limits have therefore been encountered for conventional wind tunnels.

Some years ago, H. Ludwieg suggested in a different context a device which now appears to be remarkably well suited for this kind of application (5). The device consisted of a long cylindrical tube as a container for the compressed air. One end of the tube was closed; the other end contained a supersonic nozzle, a test section and a quick opening valve which was opened to the atmosphere. Modifications of this arrangement are possible and in the Yale University Ludwieg tube (6) a conventional shock-tube is altered by the insertion of a supersonic nozzle into the section upstream of the diaphragm (the high pressure section). After the diaphragm breaks, a shock wave and a contact surface travel downstream, and the head of the expansion wave moves upstream through the supersonic nozzle. After the remaining part of the expansion wave is swept back downstream, stable conditions of supersonic flow are maintained in the nozzle until the reflected expansion wave returns to the throat. The operating stages for this intermittent tube wind tunnel (also known as the "Ludwieg tube") are indicated in Figure 1, a $t - x$ diagram with a sketch of the tube. When the diaphragm is ruptured, a centered expansion wave is formed and moves upstream into the high pressure tube where the gas is at the initial conditions denoted by 4. Part of it passes through the nozzle and travels to the end of the high pressure tube where it is reflected and returns to the nozzle. This marks the end of the first steady flow period. Simultaneously with the diaphragm breakage a shock wave is formed and travels downstream into the dump tube followed by the contact surface. Here the initial undisturbed conditions of the gas are denoted by 1. The times shown in Figure 1 are t_i , the total starting time; t_{i1} , the time required to establish sonic conditions at the nozzle's throat; and t_T , the total time of stable supersonic flow. In the literature, one can find derivations of the equations relating the nozzle parameters to the initial conditions in the tube. In these analyses, it is generally assumed that the nozzle has zero length, that the flow is one-dimensional and inviscid,

and that one is dealing with a perfect gas, as shown, e.g., by Cable and Cox (7) and Becker (8). With this device, high stagnation pressures can be maintained in the high pressure side and steady supersonic flow of relatively short but useful duration can be established in the test section. Furthermore, an important practical advantage, with respect to high pressure blow-down tunnels, arises from the fact that no valves are required to maintain steady nozzle supply conditions. For these reasons, interest now exists in the Ludwieg tube and in its possible application.

Since model and sting stresses are a limiting factor in the capabilities of a tube wind tunnel, it is important to know what the stress on a model will be during a test. Steady state stresses can be predicted fairly well based on previous measurements of drag and lift coefficients. However, the loads on a model during the starting process are not as well known. Thus, it is important to be able to predict what the starting loads on a model will be, and whether or not they are larger than the steady state loading. Understanding the starting stage of a Ludwieg tube is, therefore, necessary if one wants to predict the starting loads to which a model will be subjected.

With regard to the starting stage, that is, the elapsed time between the rupture of the diaphragm, or the opening of a valve, and the establishment of steady supersonic flow in the nozzle, some uncertainties have persisted. First, there is the question of whether or not starting shock waves are produced after sonic conditions are obtained at the throat of the nozzle. Such shocks may originate at the throat and travel downstream through the nozzle prior to the steady flow stage, and may have adverse effects on the model. In addition, there is the question of how, in fact, the steady state parameters in the nozzle are acquired. In a previous investigation of the starting processes in another type intermittent wind tunnel, with a closed jet nozzle-test section geometry, Bull (10) observed starting shocks and flow separation in the diverging section of the nozzle. He stated that this was caused by the adverse pressure gradient in the nozzle resulting from the reflected part of the initial expansion wave. From the results of a study of the starting process in the Yale Ludwieg tube with a different type of nozzle-test section configuration (semi-open jet nozzle), Johnson and Cagliostro (11,12) showed that no starting shocks occurred during the starting period. Therefore, the nozzle and test section geometry may have significant effects on the wave phenomena and flow patterns that occur during the starting phase.

The objective of the current research program on the starting process of the Ludwieg tube is to determine

experimentally the effects of nozzle geometry and configuration on the starting process with respect to the presence or absence of shock waves, flow separation and the time to reach a steady state in the nozzle and test section. The experimental techniques used are spark and high-speed movie shadowgraphy, streak interferometry, and transient pressure measurements. Both the semi-open jet and the closed jet nozzle-test section configurations are investigated.

In this report we shall present further results from our observations of starting processes in a supersonic Ludwig tube.* We are concerned at this point only with experimentally determining what appear to be the gross qualitative features of this starting phase.

* Previous results have been given in References 11 to 14.

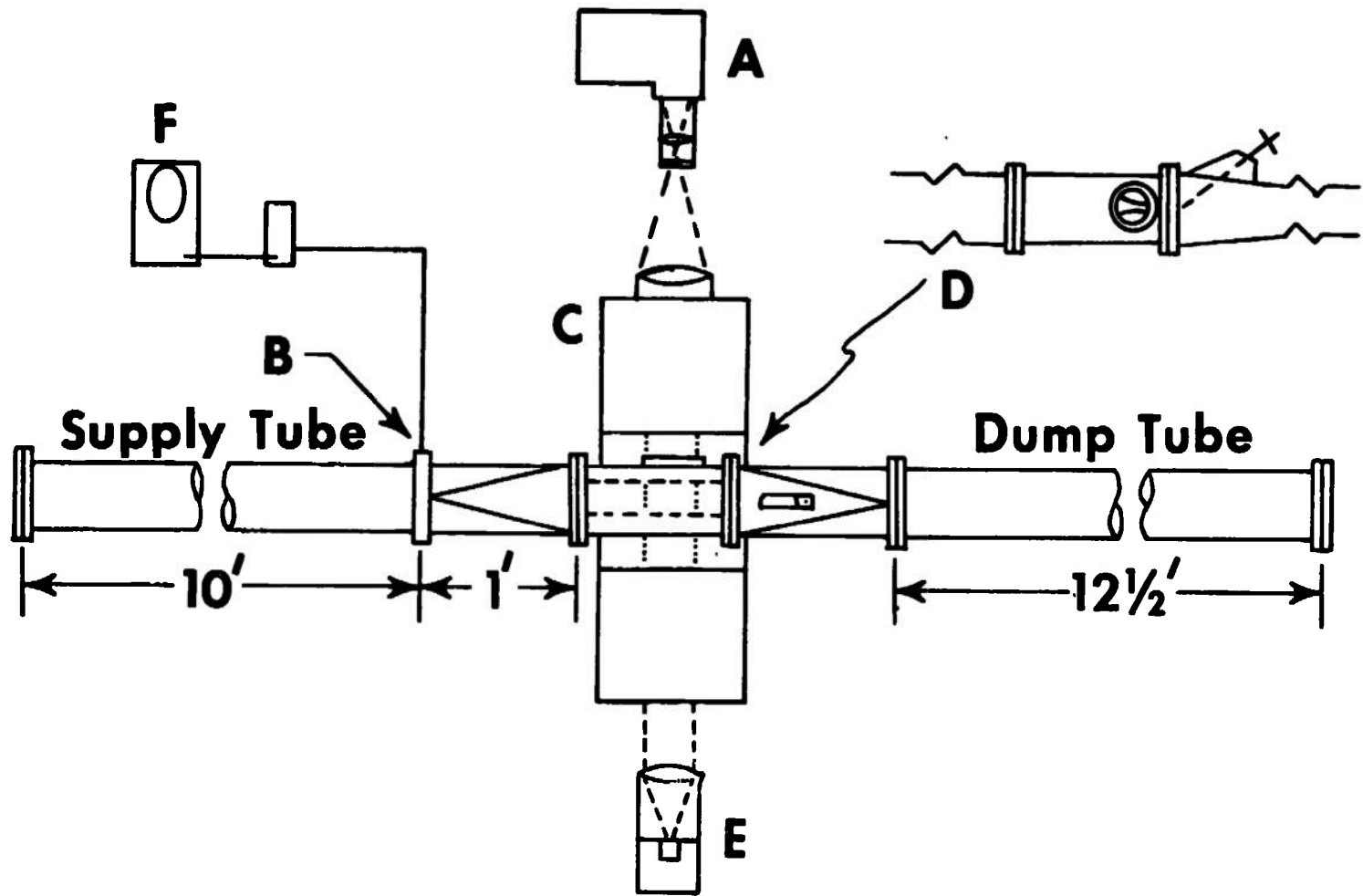


Fig. 2 Experimental Apparatus. (A) High Speed Camera. (B) Pressure Transducer (at upstream position). (C) Mach-Zehnder Interferometer. (D) Side View of Test Section. Supply tube: 5.30 in. I.D. Dump tube: 3.76 in. I.D. Nozzle: 2" x 2" at throat ($M = 1.67$ at exit). (E) Collimating Lens and Light Source. (F) Oscilloscope to record pressure traces.

II

EXPERIMENTAL APPARATUS

The Yale University Ludwieg tube (6) is sketched in Figure 2. Its over-all length is 26 ft., and a diaphragm can be placed on either side of the test section. However, in this report only results of the downstream location will be given. Four two-dimensional nozzles were used in this study as designated Y160, Y167, Y250, and Y300 with exit Mach numbers of $M = 1.60, 1.67, 2.50, \text{ and } 3.00$ respectively. The Y167 and Y300 are continuously expanding nozzles. The Y167 is a wedge-type nozzle with a three degree half angle expansion and a six inch radius of curvature at the throat, and the Y300 is a cubic profile nozzle. The Y160 and Y250 are parallel flow nozzles*. The nozzles can be placed at various positions in the 1.5 ft test section. Extension blocks for each nozzle were used to convert the nozzles from the semi-open jet to the closed jet configuration. Two sections immediately upstream and downstream of the test section respectively produce a smooth transition from the circular supply and dump tubes to the rectangular test section. In all experiments, the operating gas was dry air.

Three diagnostic techniques have been used in our investigations:

(1) Timed shadowgraphs are made during the starting stage. High-speed movie shadowgraphs with a 0.22 msec frame to frame sampling rate are taken using a Fastax camera. Spark shadowgraphs are taken at various time intervals during the starting process using a 1 μ sec 10,000 volt spark source.

(2) Slit streak-interferometry is used to obtain density measurements as a function of time on the nozzle center line. In this method a horizontal slit is placed between the light source and the collimating lens so that its image appears at the test section with a width of 2mm. This dimension together with the equivalent film speed of a streak camera of 300m/sec, gives a time resolution of roughly 7 μ sec. The Zeiss Mach-Zehnder interferometer (plate size; 4 1/8" x 7") is adjusted so that the image of vertical interference fringes appears at the center of the test section. With the rotating prism in the Fastax movie camera removed and with the film moving in a vertical plane, continuous interferograms are obtained which allow one to follow the movement of each fringe, thus permitting a determination

* These are the nozzles designed at the U.S. Naval Ordnance Laboratory.

of the change in density with time at any position along the centerline of the nozzle. Shock waves would be noticeable as discontinuities in the fringe pattern. The increase and decrease in density can be determined according to the direction of motion of the fringes. The entire system is found to be sensitive to density changes of less than 1.0% with the compensating chamber properties arranged to duplicate the critical density in the nozzle.

(3) Static pressure measurements have been made in the supply tube and at various locations in the nozzle using two calibrated high speed 3 μ sec rise-time quartz pressure-transducers (Kistler, Model #606L).

For a more detailed description of the tube wind tunnel, the nozzles and auxiliary equipment, see Appendix I.

III

EXPERIMENTAL RESULTS

Spark shadowgraph photography, transient pressure recording, high-speed movie shadowgraph photography, and high-speed streak interferometry were the diagnostic techniques used here to study the starting processes in the Yale Ludwig tube. Dry air at room temperature ($23.0 \pm 1.0^\circ\text{C}$) was used in both the supply and dump tubes. The initial supply pressure was two atm except for experiments with models in the test section, in which case the pressure was one atm. The lower pressure was used to reduce loading on the model and sting. The initial pressure ratio, P_4/P_1 , was 10.0 for the Y160 and Y167 nozzles and 30.0 for the Y250 and Y300 nozzles to insure that the flow was completely expanded in the nozzle and test section during the first steady flow period. Three sheets of cellophane each about 0.002 in. thick were used for the diaphragm. Diaphragm breaking time was measured to be less than 0.1 msec.

The experimental results show that the nozzle-test section configuration, i.e., semi-open jet or closed jet, has a significant effect on the starting process in the Yale Ludwig tube. Starting shock waves were not present in the semi-open jet configuration but did appear in the closed jet configuration for the Y160 and Y167 nozzles. In the Y250 and Y300 nozzles, flow separation and the formation of complex oblique shock patterns occurred during the starting process with each nozzle configuration. The presence of a model in the test section did not noticeably effect these results, however it did cause an increase of about 100% in the starting time in the Y167 nozzle in the closed-jet configuration.

The effects of the nozzle configuration on the starting process are evident from the experiments with the Y160 and Y167 nozzles. Figure 3 shows prints of film strips from high-speed shadowgraph movies of the starting process in the Y160 nozzle in the semi-open jet and the closed jet configuration. Also shown is a film strip with the wedge model at the exit of the semi-open jet nozzle. The time elapsed between each frame is about 0.22 msec and the flow is from left to right. The field of view shows the nozzle throat at the left and three inches downstream from the throat. In the semi-open jet configuration, no starting shock waves form in the nozzle or pass over the model. In the closed jet configuration, a steep pressure wave forms in the nozzle downstream of the nozzle throat. It moves downstream, strengthens and becomes a shock wave. The shock continues to move downstream to the end of the field of view. Upstream of the shock wave the flow is steady. Note the shock wave

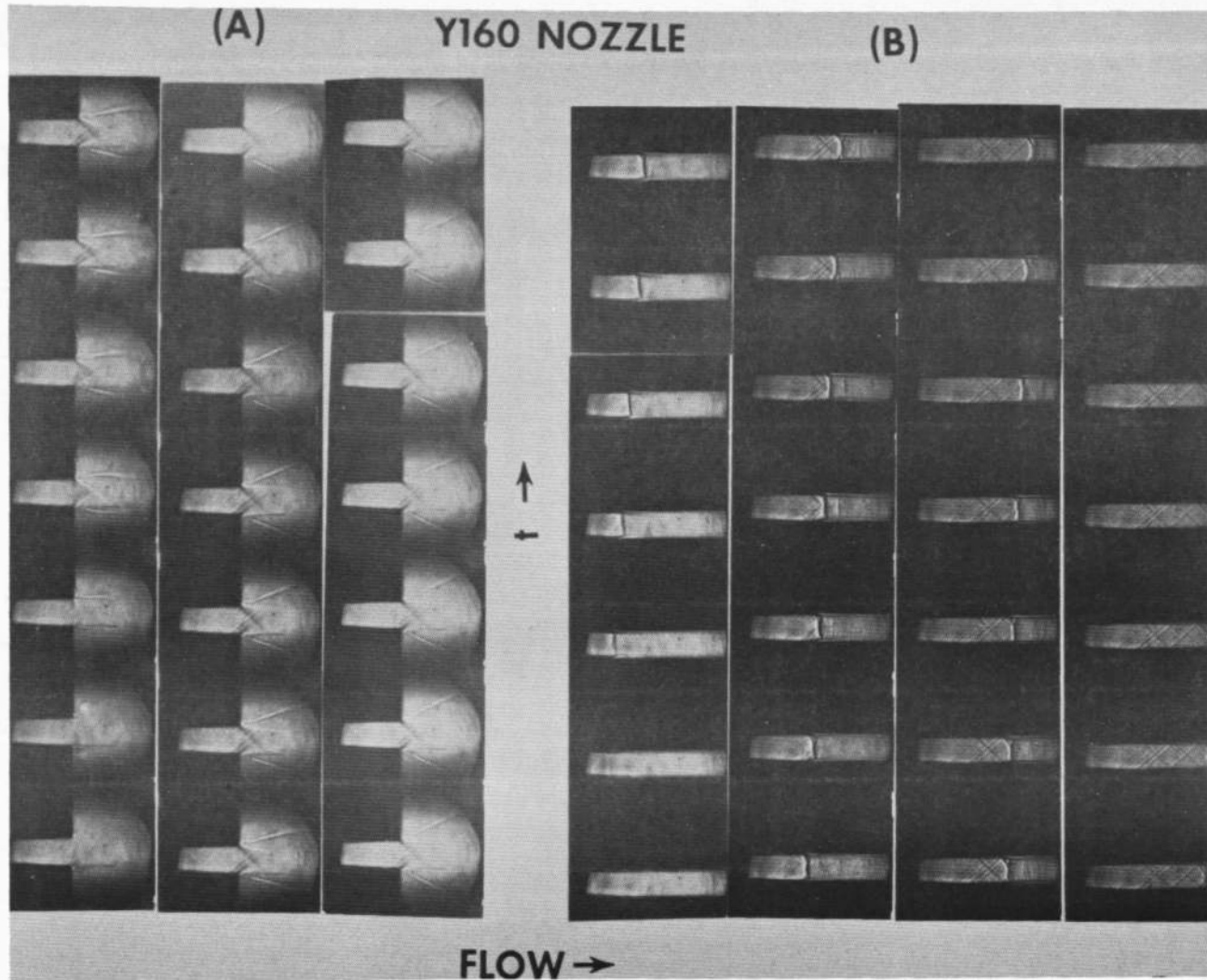


Fig. 3 Shadowgraph High-Speed Movie Prints of Starting Process in the Y160 Nozzle, (A) Semi-Open Jet, (B) Closed Jet, (C) Semi-Open Jet with a Wedge Model at Nozzle Exit. The time between each frame is about 0.22 msec; field of view shows nozzle throat at left and three inches downstream. Flow is from left to right.

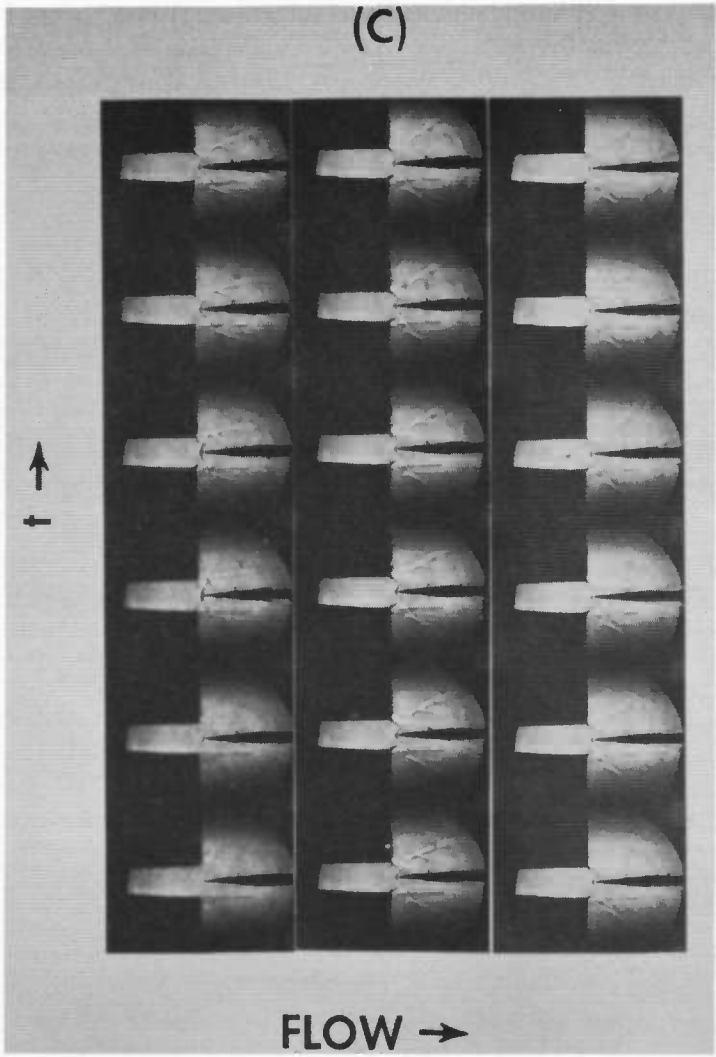


Fig. 3 Concluded

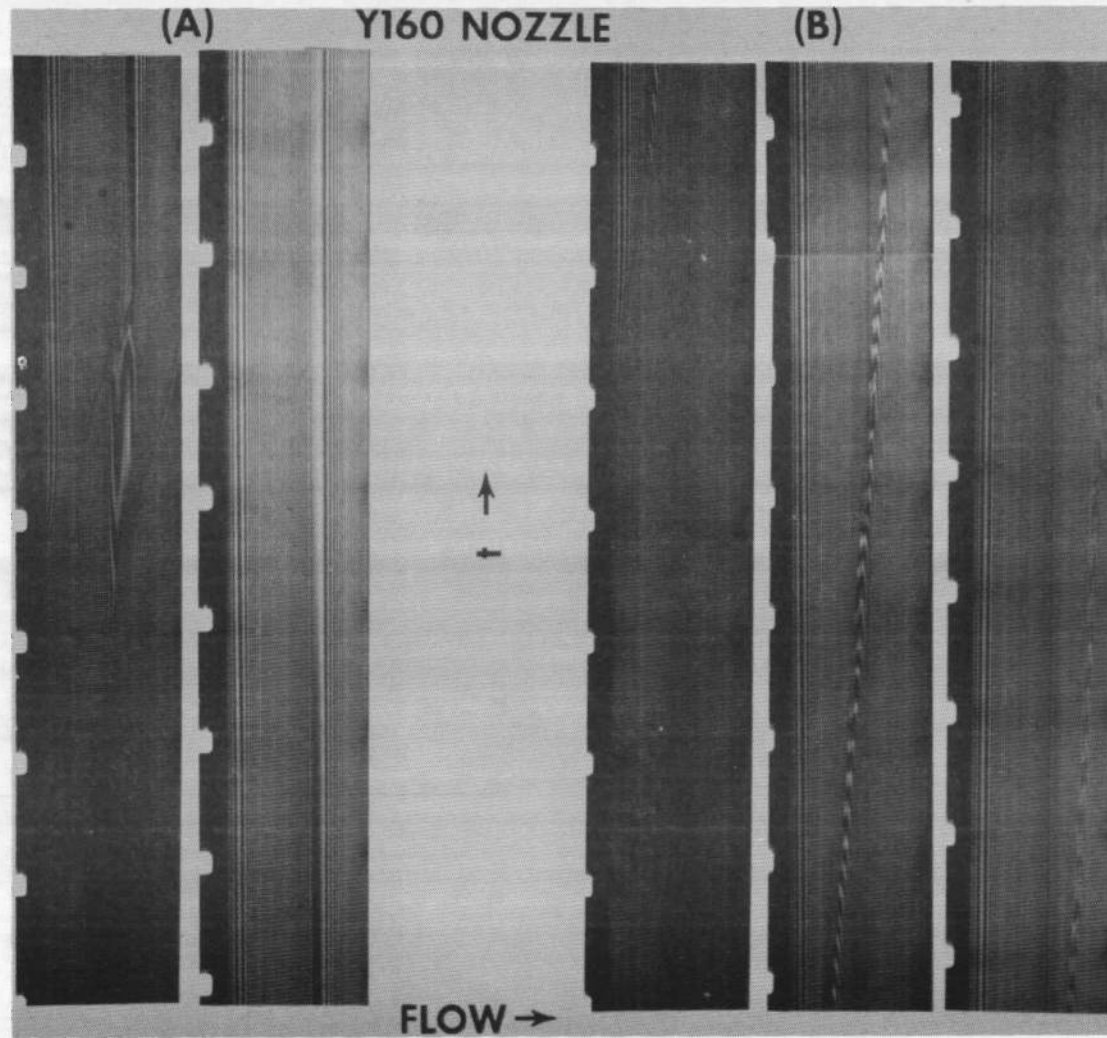


Fig. 4 Streak Interferograms of Starting Process in the Y160 Nozzle, (A) Semi-Open Jet and (B) Closed Jet. The t and x axes are shown; field of view is nozzle throat at left and three inches downstream. Decreasing densities are indicated by the motion of fringes from left to right.

and boundary layer interaction. A comparison of streak interferograms made during the starting period in the same nozzle in the semi-open jet and closed jet configuration is shown in Figure 4. Here time increases in the upward vertical direction and flow is from left to right. The nozzle throat is at the left and the field of view is three inches. At time zero, the gas is at rest and the density is equal to its initial value, ρ_4 . The initial fringe distribution is set for vertical fringes. When the diaphragm is ruptured, the initial expansion wave travels upstream from the diaphragm location and lowers the density of the gas in the nozzle and test section. This density decrease is indicated by a shifting of the interference fringes to the right. Positive density gradients in the flow direction appear as an increase in the fringe density, i.e., the number of fringes per unit length, over the initial fringe distribution, and a negative density gradient appears as a decrease in the fringe distribution. In the semi-open jet case, there is no starting shock wave, although a positive density gradient appears. The nozzle exit is at the center of the interferogram. In the closed jet case the density gradient appears to increase downstream of the nozzle throat and to steepen into a shock wave. The path of the shock wave is clearly indicated in the interferogram as the change in position of the steep density gradient which moves downstream.

The density along the Y160 nozzle centerline for various times during the starting process is shown in Figure 5, for the semi-open jet and closed jet configurations. There is a significant difference between the density distributions in each case. In the semi-open jet configuration the density gradient does not become as positive as it does in the closed jet configuration. The adverse pressure gradient in the direction of flow seems to cause the boundary layer to thicken, as can be seen in the high-speed shadowgraph movie prints in Figure 3. In the closed jet configuration the density gradient increases with time and finally appears to steepen into a shock wave which continues to move downstream. Similar results were found from the spark shadowgraph pictures of the starting process in the Y167 nozzle for the semi-open jet and closed jet configuration which are shown in Figure 6. The exit of the nozzle is located at the center of each picture and the flow is from left to right. The pictures show 3.6 inches of the flow in the horizontal direction. These show no shock waves formed in the nozzle during the starting process for the semi-open jet configuration. However, clear pictures of a shock wave formed during the starting process for the closed jet configuration are seen with noticeable shock wave-boundary layer interaction. Similar spark shadowgraph pictures of the starting process with a model present as

Y160 Nozzle

Times (msec): $t_a = 0.0$, $t_b = 0.6$, $t_c = 0.8$, $t_d = 1.0$, $t_e = 1.4$,

$t_f = 1.5$, $t_g = 1.8$, $t_h = 2.0$, $t_i = 2.2$, $t_j = 2.5$

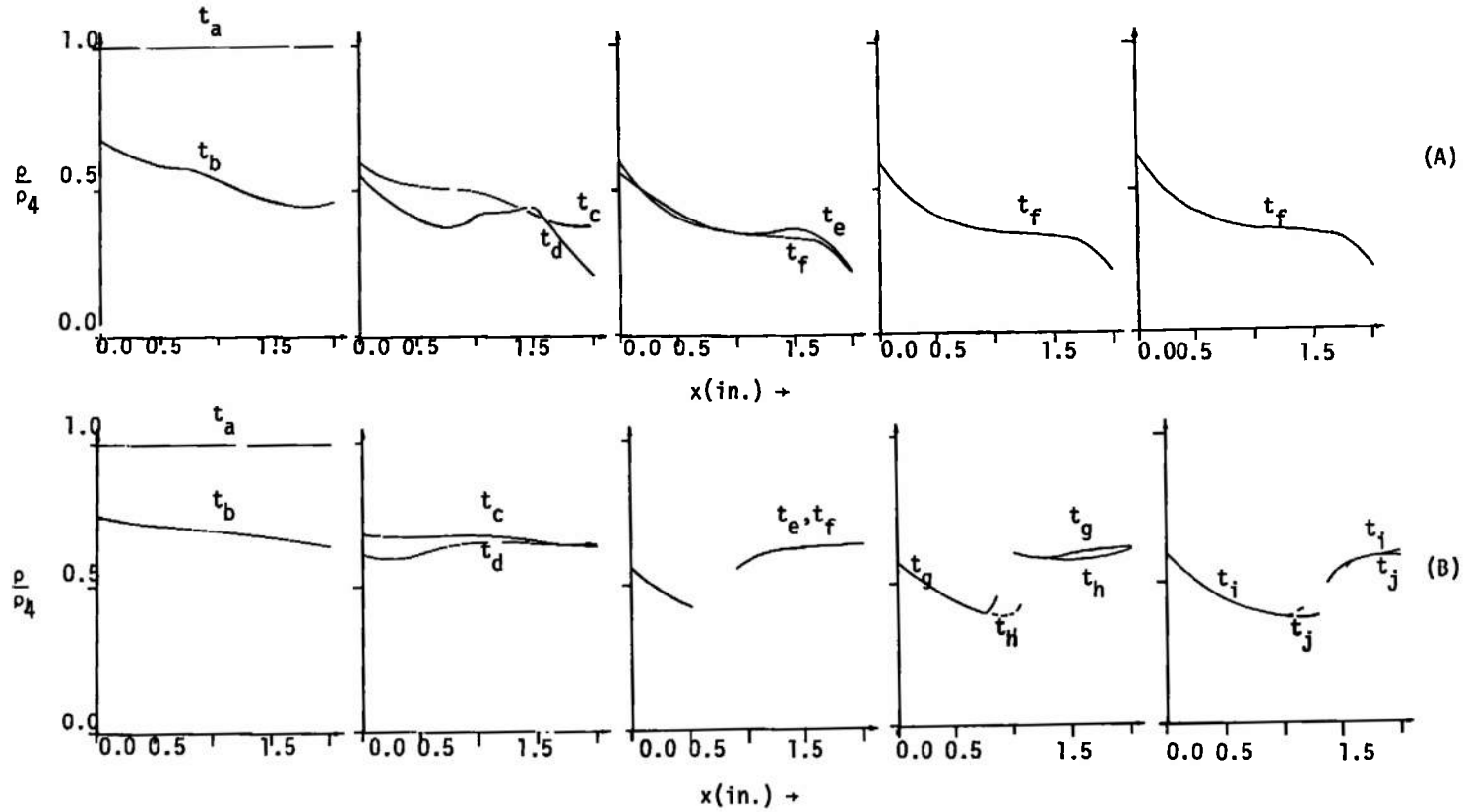


Fig. 5 Density Measurements in Y160 Nozzle, (A) Semi-Open Jet and (B) Closed Jet Configuration. The density along 2.0 inches of the nozzle centerline starting at the nozzle throat, $x = 0.0''$ is shown for various times during the starting stage.

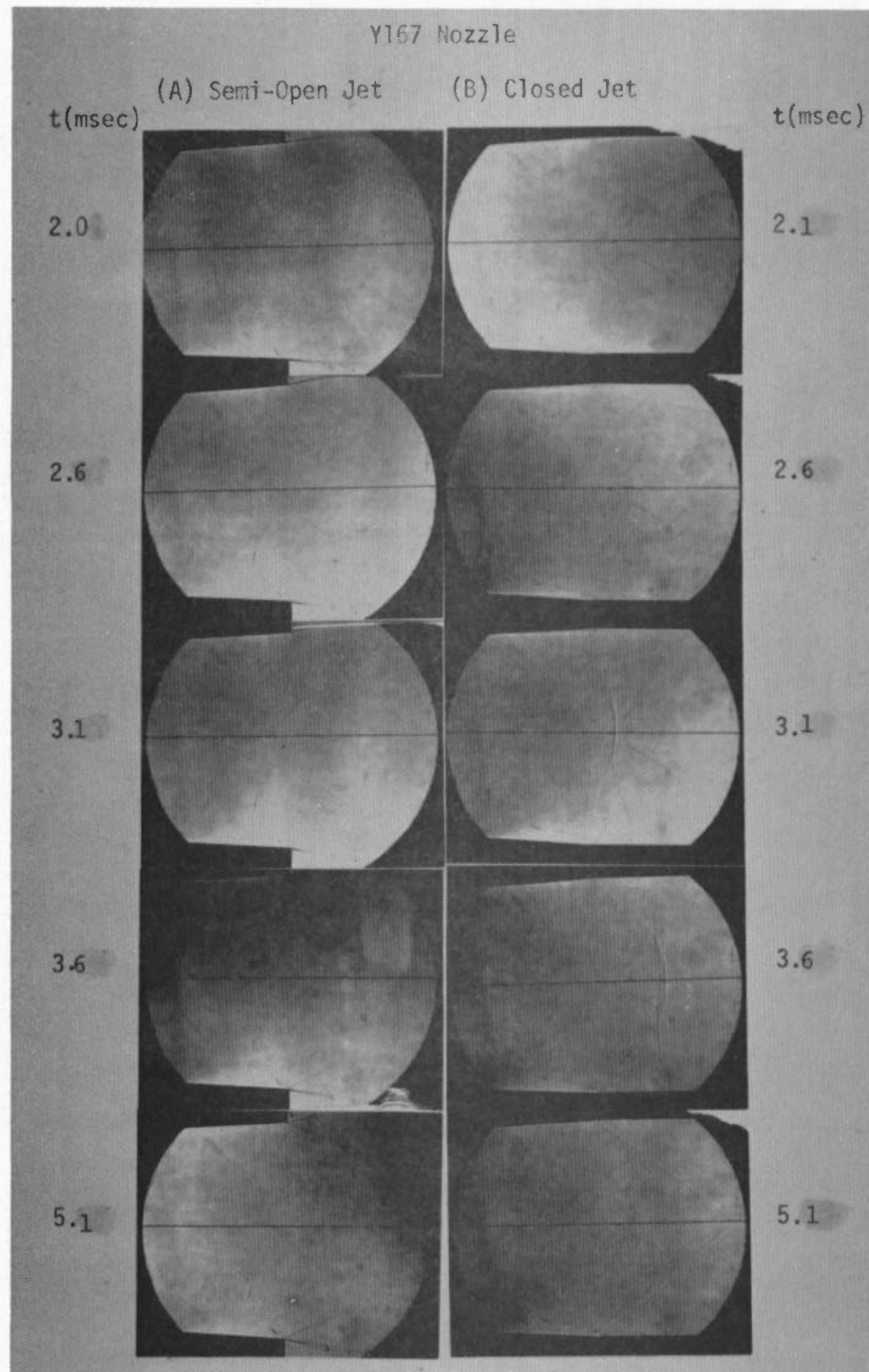


Fig. 6 Spark Shadowgraph Pictures of the Starting Process in the Y167 Nozzle, (A) Semi-Open Jet, and (B) Closed Jet Configuration. Field of view is 3.6 inches in flow direction, i.e., from left to right, with the nozzle exit at the center. Times are measured from diaphragm rupture time which is at $t = 0.0$.

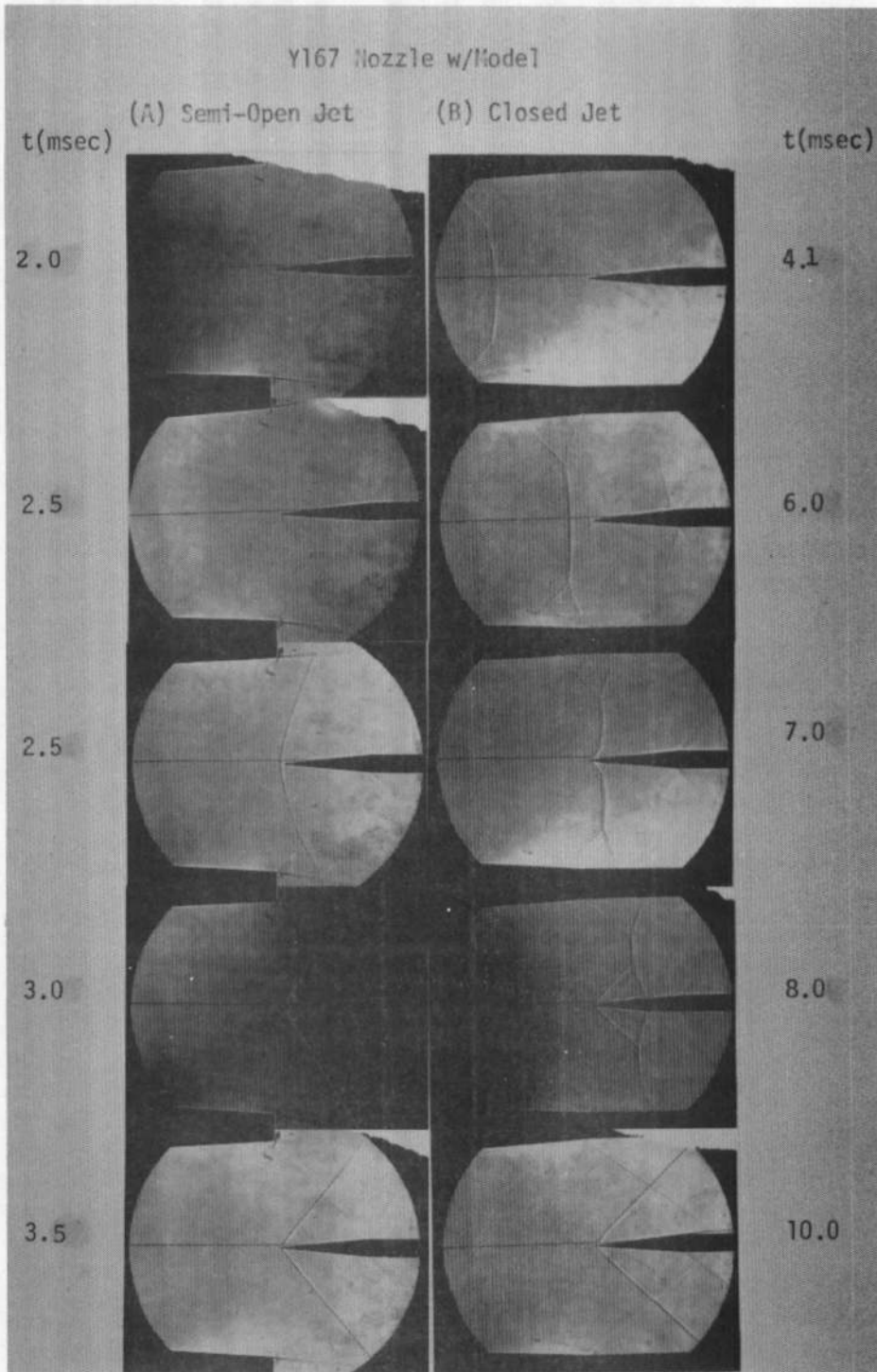


Fig. 7 Spark Shadowgraph Pictures of the Starting Process in the Y167 Nozzle with a Wedge Model at Nozzle Exit, (A) Semi-Open Jet, and (B) Closed Jet Configuration. Field of view is 3.6 inches in flow direction, i.e., from left to right, with the nozzle exit at the center. Times are measured from diaphragm rupture time which is at $t = 0.0$.

seen in Figure 7 show that the model has no significant effect on the presence of starting shock waves.

The difference between the starting process in the semi-open jet and the closed jet configuration can be seen in these pictures. Note that in the former configuration steady flow occurs about the model uniformly and that the shock wave formed in front of the model is caused by the model and therefore does not pass by the model. In contrast in the closed jet configuration the shock is a starting shock which forms during the starting process whether or not there is a model present. Unlike the shock wave which appears in front of the model in the semi-open jet case, this shock wave passes over the model leaving a steady supersonic flow upstream of the model. Here the final steady flow at a position about the model occurs discontinuously as the shock wave passes by it.

Flow separation occurs during the starting process in the higher Mach number Y250 and Y300 nozzles. Prints from high-speed shadowgraph movie strips of the starting process in the Y250 nozzle in the semi-open and closed jet are shown in Figure 8 with the flow from left to right and 0.22 msec separation of frames. The field of view is 3.0 inches. These pictures show that flow separations and patterns of oblique shocks occur during the starting process for both configurations. The presence of a model appears to have no effect on the starting process here. Note that unlike the symmetrical starting process in the Y160 and Y167 nozzles, the flow field in these nozzles during the starting process may become unsymmetrical. A set of spark shadowgraph pictures for the Y300 nozzle show similar results for the starting process and are shown in Figure 9. Again note that flow separation and oblique shock waves occur during the starting process. The flow separation may be due to adverse pressure gradients similar to those which occurred in the Y160 nozzle.

Transient pressure traces taken at various locations along the nozzle centerline during the starting process show the pressure variation with time at fixed positions. Examples of such results for the Y167 and Y300 nozzles are shown in Figures 10 and 11. These oscilloscope traces represent the pressure along the y-axis and the time along the x-axis with the scales shown. For the Y167 nozzle, at position C (see Figure I.2 in Appendix I), in the subsonic section of the nozzle, the pressure decreases and "undershoots" its final steady state value during the starting stage. At position D, downstream of the nozzle throat, the pressure again undershoots its steady state value, but by a smaller amount. Note also that the pressure gradient with respect to time is not as steep as at position C.

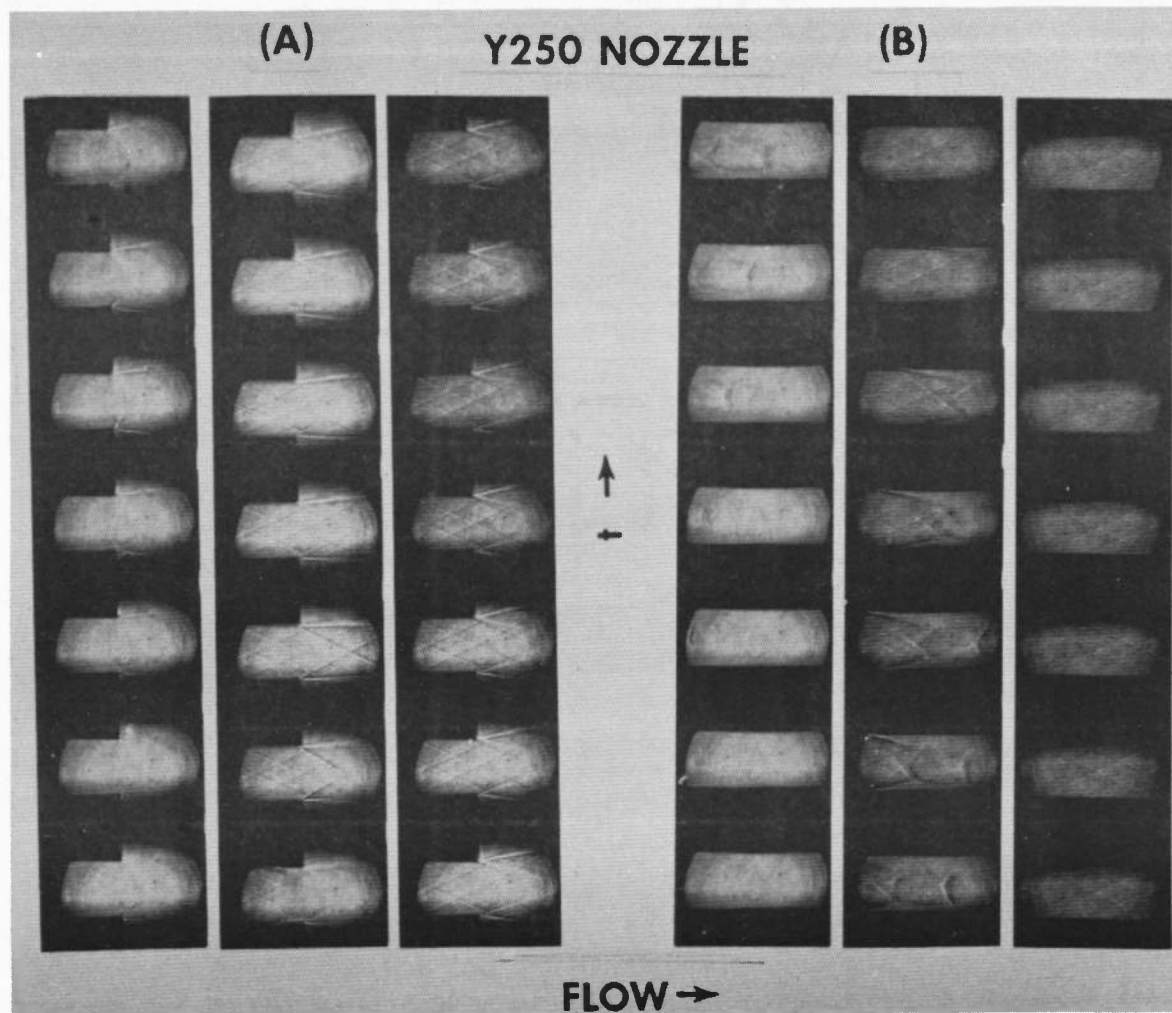


Fig. 8 Shadowgraph High-Speed Movie Prints of Starting Process in the Y250 Nozzle, (A) Semi-Open Jet, (B) Closed Jet, (C) Semi-Open Jet with Model, and (D) Closed Jet with Model. The time between each frame is about 0.22 msec; field of view is 3.0 inches in flow direction, i.e., from left to right with the nozzle exit at the center.

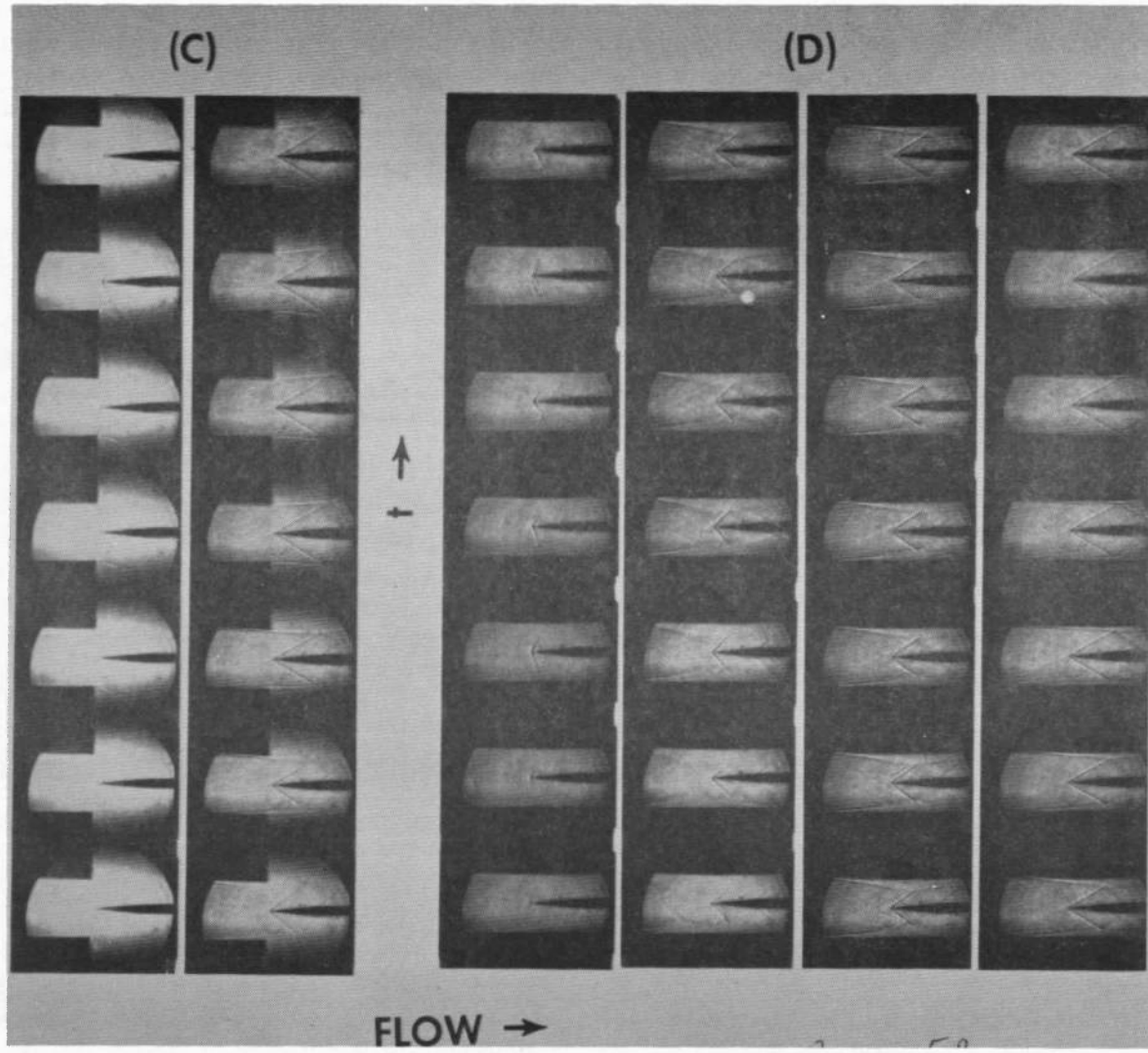


Fig. 8 Concluded

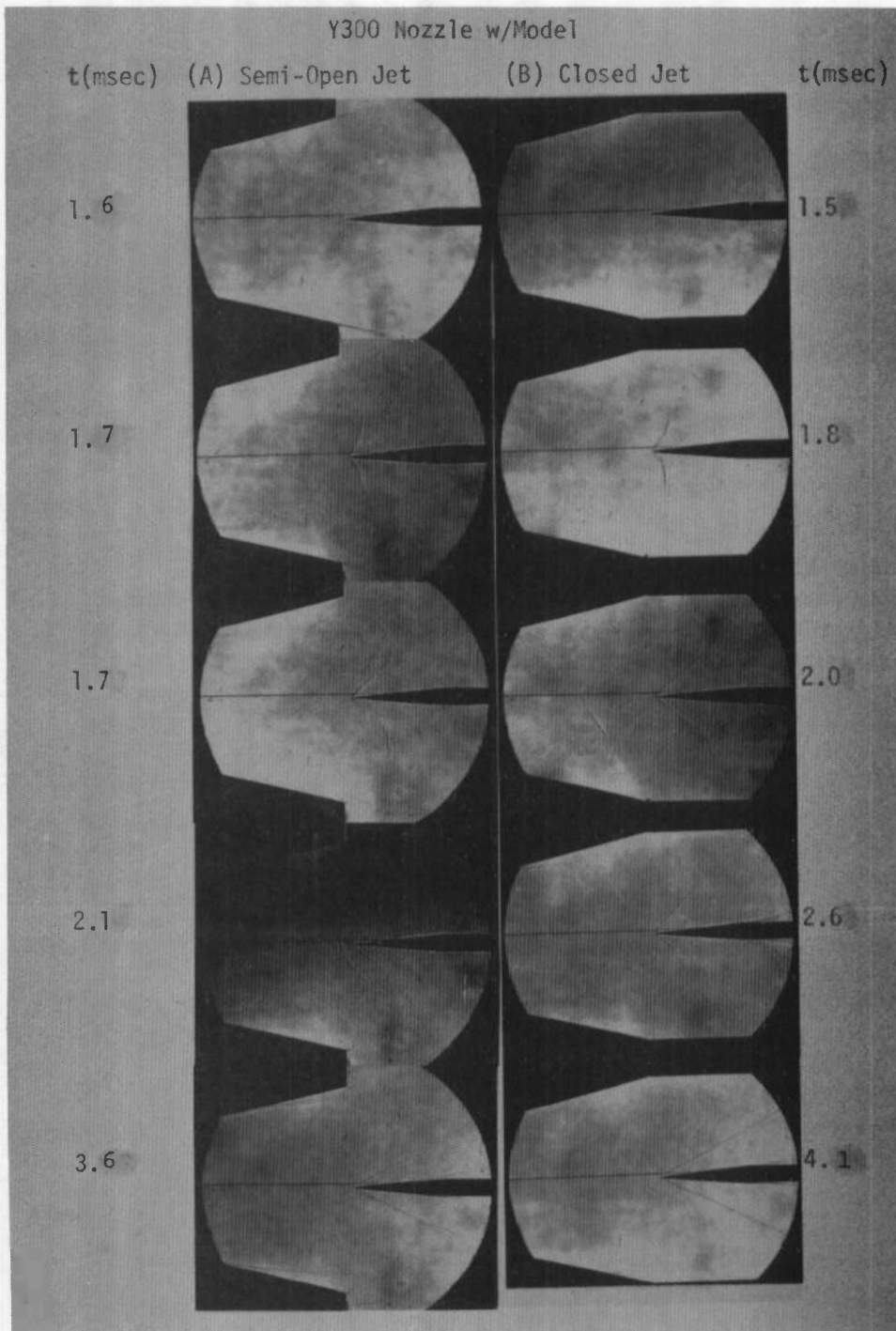


Fig. 9 Spark Shadowgraph Pictures of the Starting Process in the Y300 Nozzle with a Wedge Model at Nozzle Exit, (A) Semi-Open Jet, and (B) Closed Jet Configuration. Field of view is 3.6 inches in flow direction, i.e., from left to right, with the nozzle exit at the center. Times are measured from diaphragm rupture time which is at $t = 0.0$

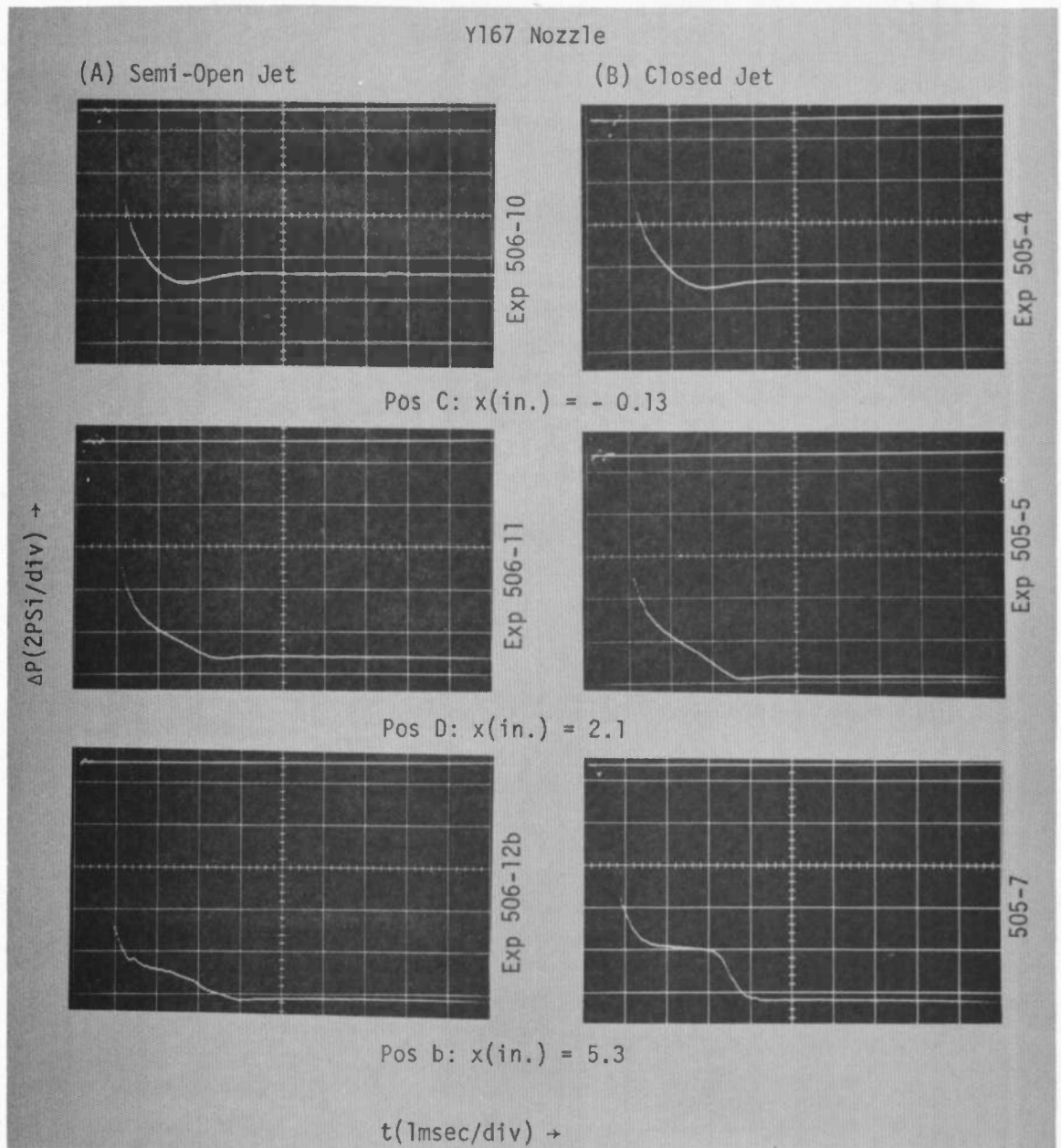


Fig. 10 Pressure Measurements in the Y167 Nozzle, (A) Semi-Open Jet, and (B) Closed Jet Configuration. Positions are measured from nozzle throat in downstream direction; $P_4 = 1.0$ atm. Pressure trace is triggered at diaphragm rupture.

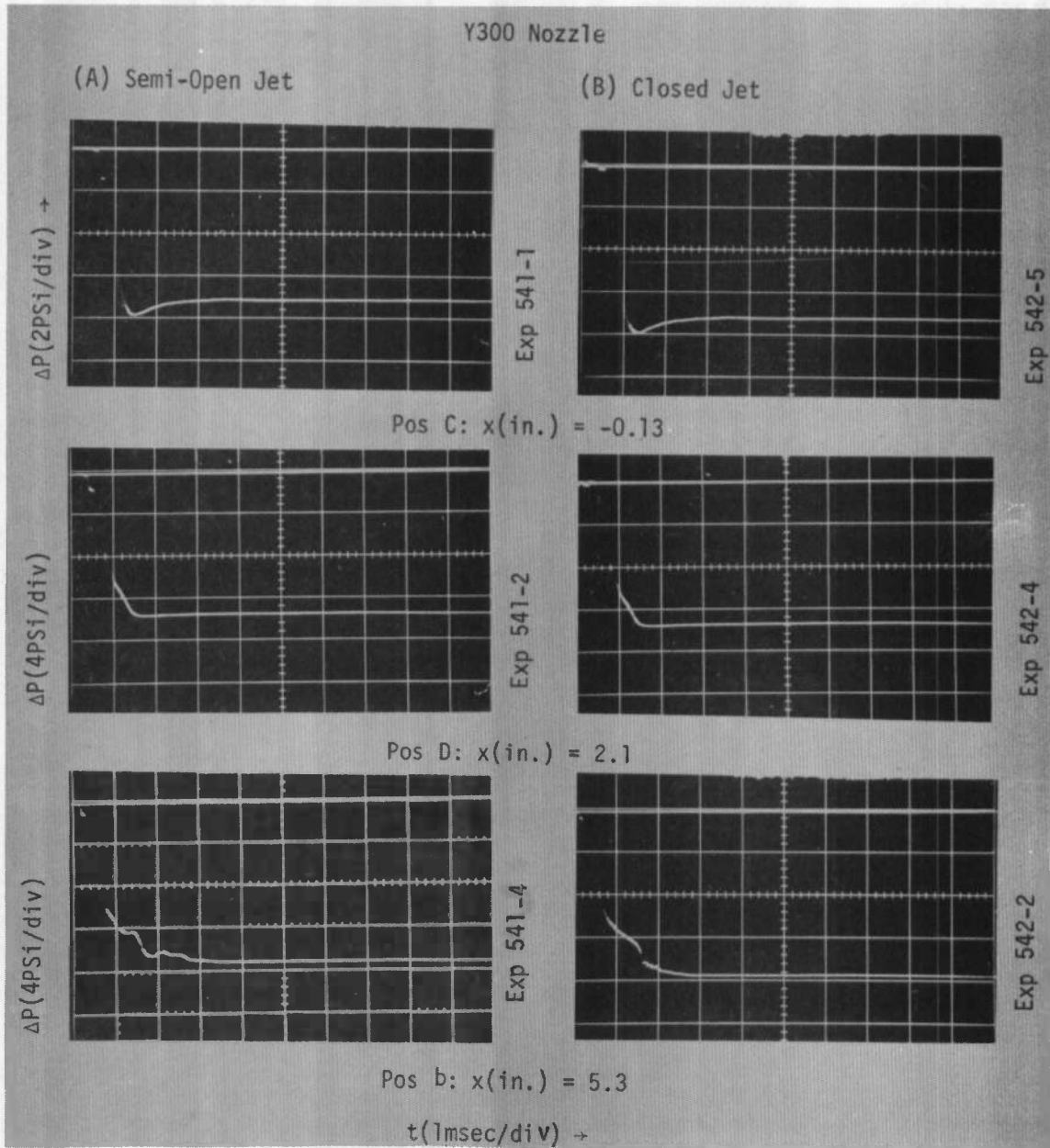


Fig. 11 Pressure Measurements in the Y300 Nozzle, (A) Semi-Open Jet, and (B) Closed Jet Configuration. Positions are measured from nozzle throat in the downstream direction; $P_4 = 1.0$ atm. Pressure trace is triggered at diaphragm rupture.

At position b, the shape of the pressure traces for the closed jet configuration differ appreciably. The steep drop in pressure, which appears in the trace for the closed jet configuration, may be compared with the drop in density shown in Figure 12. Here the density was measured from a streak interferogram of the starting process in the Y160 nozzle in the closed jet configuration. Similar results were seen from pressure traces made during the starting process in the Y300 nozzle.

Starting times* measured from the pressure traces are tabulated in Table 1 for the Y167 and Y300 nozzles. The starting time for the Y167 nozzle in the closed jet configuration is affected significantly by the presence of the model. Without a model in the test section, there was no noticeable difference in the starting times between the semi-open jet and the closed jet configuration.

* This is defined as the time to establish constant pressure at the transducer location after the initial expansion fan arrives.

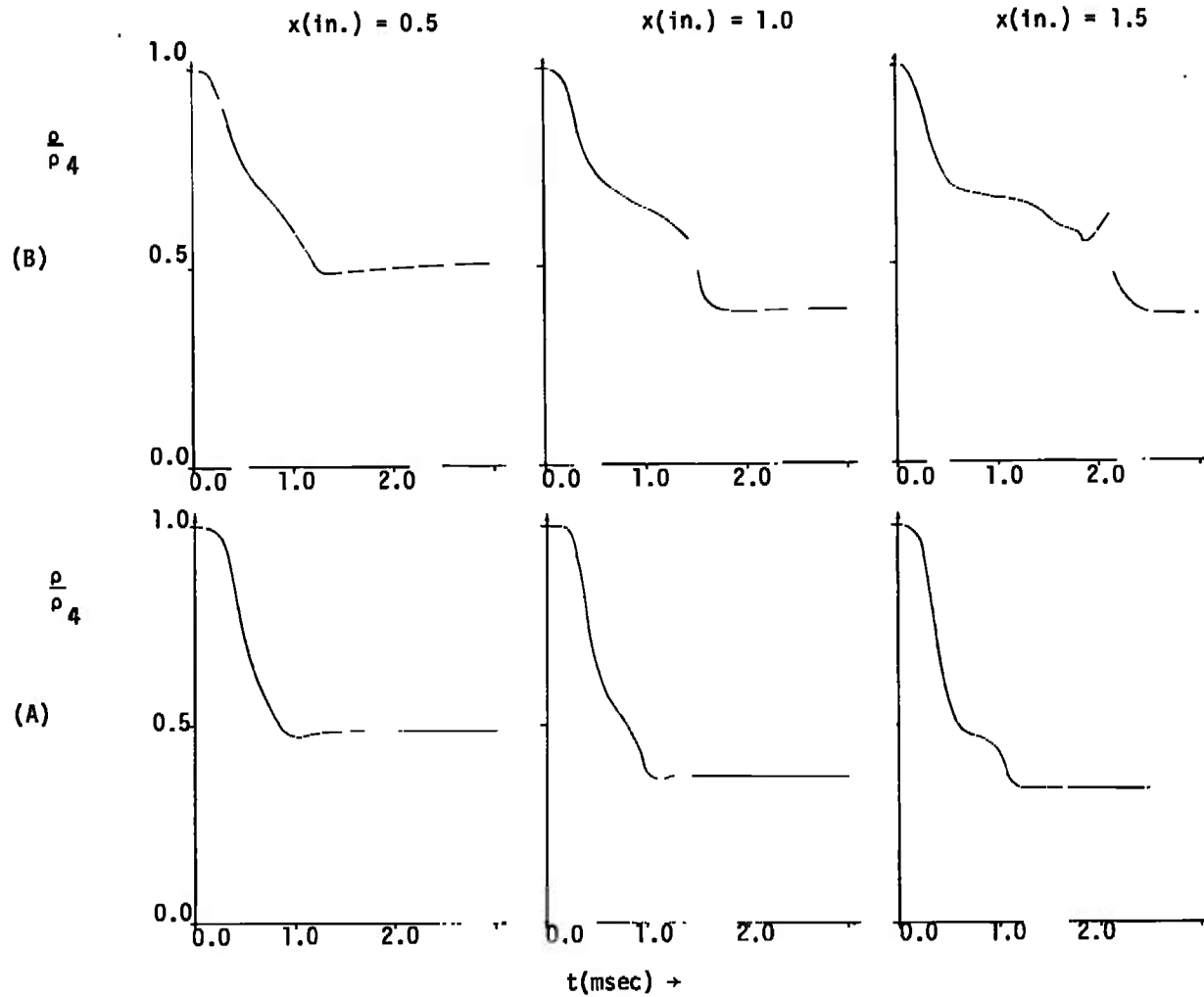


Fig. 12 Density Measurements in the Y160 Nozzle in the (A) Semi-Open Jet and (B) Closed Jet Configuration. Positions are measured from the nozzle throat in the downstream direction; $P_4 = 2.0$ atm. Time starts when initial expansion fan reaches a position 3.6 in. downstream from nozzle throat.

TABLE I

Starting Times for the Y167 and Y300 Nozzles in the Semi-Open Jet and Closed Jet Configurations. Times were measured from the pressure traces made at positions along the nozzle centerline. The positions are measured from nozzle throat in the downstream direction. Times start when expansion fan reaches pressure transducer. Gas: Dry Air. Initial pressure: P4 = 1.0 atm.

Position x (in.)	Nozzle Configuration	Y167 Nozzle		Y300 Nozzle	
		Exp. No.	Starting Time (msec)	Exp. No.	Starting Time (msec)
-0.13	Closed Jet, w/o Model	505-4	4.9	542-5	4.0
-0.13	Semi-Open Jet, w/o Model	506-10	4.0	541-1	4.0
-0.13	Closed Jet, w/ Model	507-6	4.9	543-1	4.0
-0.13	Semi-Open Jet, w/ Model	508-11	4.0	540-5	4.1
2.1	Closed Jet, w/o Model	505-5	3.6	542-4	3.5
2.1	Semi-Open Jet, w/o Model	506-11	4.0	541-2	3.0
2.1	Closed Jet, w/ Model	508-10b	4.2	543-2	3.5
2.1	Semi-Open Jet, w/ Model	507-5	4.0	540-4	3.5
5.3	Closed Jet, w/o Model	505-7	4.1	542-2	3.0
5.3	Semi-Open Jet, w/o Model	506-12b	4.0	514-4	3.5
5.3	Closed Jet, w/ Model	508-5b	9.4	543-4	3.5
5.3	Semi-Open Jet, w/ Model	507-4	4.0	540-2	4.0

IV

DISCUSSION OF RESULTS

For the flow conditions and nozzle geometries investigated, it has been shown that the starting process in the Yale Ludwig tube depends significantly on the nozzle-test section geometry and configuration.* In particular, starting shock waves appear in the Y160 and Y167 nozzles in the closed jet configuration, and do not appear when the same nozzles are used in the semi-open jet configuration. Flow separation appeared in the higher Mach number nozzles, Y250 and Y300, during the starting process. These results are especially important since the flow patterns during the starting process usually are the determining factors in the design of models and sting supports. The absence of starting shocks and of flow separation would reduce the transient loading on models during the starting process and thus lower design requirements. This would also permit the use of higher stagnation pressures in the test section, which means that higher test Reynolds numbers could be obtained. It is interesting to note that similar results were obtained with the parallel flow nozzles (Y160 and Y250) and the continuously expanding nozzles (the Y167, a wedge type nozzle with a three degree half angle expansion, and the Y300 nozzle, which has a continuously expanding cubic profile contour). The diaphragm rupturing time was less than 0.1 msec, and the time required for the head of the expansion fan to traverse the nozzle, called the "characteristic nozzle time", was about 1 msec. Therefore, the diaphragm opening process is more than one order of magnitude faster than the characteristic nozzle time. From the experimental results, we find, under geometrical conditions, the appearance of shock waves in the nozzle during the starting process. These shocks are seen if all four nozzle walls at the nozzle exit are extended by flat test section walls.

A possible explanation of the above observations follows. Moving upstream through the supersonic section of the nozzle, the initial expansion fan is partially reflected by the nozzle walls. The reflection, an expansion wave, moves downstream and causes a positive pressure gradient to appear in the flow direction. Such an adverse pressure gradient influences the development of the boundary layer (see, e.g. Ref. 9), and it causes the boundary layer to thicken. Disturbances

* Results stated here are for the particular "valve" and its location used, i.e., a cellophane diaphragm, with rupture time < 0.1 msec, located downstream of the nozzle and test section. They may not be valid for other case, in particular at largely different Reynolds numbers.

in the form of pressure waves, generated at the thickening boundary layer, add to the adverse pressure gradient further increasing its thickness. Finally pressure waves of increasing strength coalesce and form a shock wave in the supersonic flow during the starting process. These conclusions are in agreement with those of Bull (10).

The nozzle and test section geometry are related to the motion of the initial expansion wave as it moves upstream from the diaphragm location and through the nozzle. Results show that adverse pressure gradients and boundary layer thickening are less pronounced in the semi-open jet configuration as they are in the closed jet configuration. Hence, in the former configuration, noticeable boundary layer thickening, owing to increasing back pressure, and shock wave formation do not occur. A possible explanation of these results may be the following. In the semi-open jet configuration, a part of the initial expansion fan is reflected at the end of the nozzle blocks which appear in the test section as flat walls perpendicular to the flow direction. The reflected wave, an expansion wave, lowers the pressure at the nozzle exit considerably more than the initial expansion wave lowers the pressure in the nozzle. Therefore, a situation quite similar to one in which a boundary layer in a nozzle is removed by suction slits at its exit (see, e.g. Ref 9) occurs during a starting process with this pressure distribution acting along the nozzle contour and exit. Clearly, disturbances and shock waves caused by boundary layer thickening would not appear if the boundary layer were indeed removed by suction at the nozzle exit. Furthermore, this explanation suggests that, during the starting process in a nozzle with a closed jet configuration, boundary layer thickening and subsequent shock wave formation could be eliminated by using suction slits at the nozzle exit during the starting phase.* The divergence of the nozzle contours in the supersonic section of the high Mach number nozzles is greater than that in the lower Mach number nozzles, since, over given length of the supersonic section, a larger exit to throat area ratio is required in the former nozzles. This may cause steeper adverse gradients in the reflected part of the expansion wave during the starting process and, hence, cause flow separation.

The starting time did not appear to be affected much by the nozzle configuration. It was changed, however, by the presence of the wedge model in the test section, when the Y167 nozzle was used in the closed jet configuration. The ratio of the model frontal area to the test section

* Such slits could be directly connected with the dump tube.

area was about 0.075. Although this ratio was not large enough to cause blocking during the steady flow period, in line with previous experience (Ref. 15), it may have been sufficiently large to restrict the flow during the starting process. The effects of a model on the starting time in a Ludwig tube are important because the steady flow period used for model testing begins when the starting process ends. Therefore, an increase in the starting time is equal to a decrease in the test time. Shorter starting times would permit either a longer steady flow period for a given Ludwig tube, or, for the same steady flow period, a shorter supply tube.

V

SUMMARY

From experimental studies of the starting processes in the Yale Ludwieg tube wind tunnel with nozzles of final Mach numbers, $M = 1.67$, $M = 3.0$, $M = 1.6$, and $M = 2.50$, and for the range of conditions treated in our experiments, the following is found.

- (1) The starting process is significantly dependent on nozzle-test section configuration. For the $M = 1.67$ and $M = 1.60$ nozzles in the semi-open jet configuration, steady supersonic flow can be established smoothly after diaphragm rupture, without the formation of starting shocks, in about 4 milliseconds. However, in the closed jet configuration a starting shock wave forms in the diverging section of the nozzle and moves downstream to the end of the test section. The steady flow in the nozzle is terminated at the location of the shock wave. This wave moves downstream and, throughout, the flow conditions immediately following the shock are those of the final steady-state.
- (2) Flow separation occurs in the $M = 2.50$ and $M = 3.0$ nozzles during the starting process for both the semi-open and closed jet configuration. Adverse pressure and density gradients observed in the diverging section of the nozzle during the starting process appear to cause this flow separation.
- (3) Qualitative agreement with previous results for continuously expanding nozzles was obtained. The absence of starting shocks in the semi-open jet configuration was again found. As before, an "undershoot" and "overshoot" of the pressure in the supply tube and the subsonic part of the nozzle about its final steady state was observed during the unsteady starting phase.
- (4) The presence of a wedge model in the test section of the $M = 1.67$ nozzle in the closed jet configuration caused the starting time to increase by a factor of two to about 8 milliseconds. This lengthening appears to be the result of the relatively large ratio of frontal area of the model to nozzle cross section of about 0.075 for the test section Mach number of 1.67.

These results suggest that the deleterious effects arising from the interaction of starting shock waves with test models can be avoided in Ludwig tube wind-tunnels under certain conditions. Fast opening diaphragms or valves are needed and a semi-open jet issuing from the nozzles is required. When a uniform flow is required in the test section and a closed jet configuration is used, a starting shock wave may be expected to occur. Model and sting supports must be designed accordingly to withstand the higher impulsive loading. The observed boundary layer thickening and flow separation, which appeared to be caused by the measured adverse density and pressure gradients in the diverging section of the nozzle, suggest that viscous effects are important during the starting process. Therefore, this being the case, the application of suction slits at the nozzle exit for boundary layer removed during the starting phase could reduce these viscous effects. Finally, since in a larger facility which operates in the same Mach number range used here and at higher stagnation pressures ($\sim 10^3$ atm), the Reynolds numbers of about $Re/ft \sim 10^8$ are much greater than those used here, $Re/ft \sim 10^5$, viscous effects may be expected to be less important.

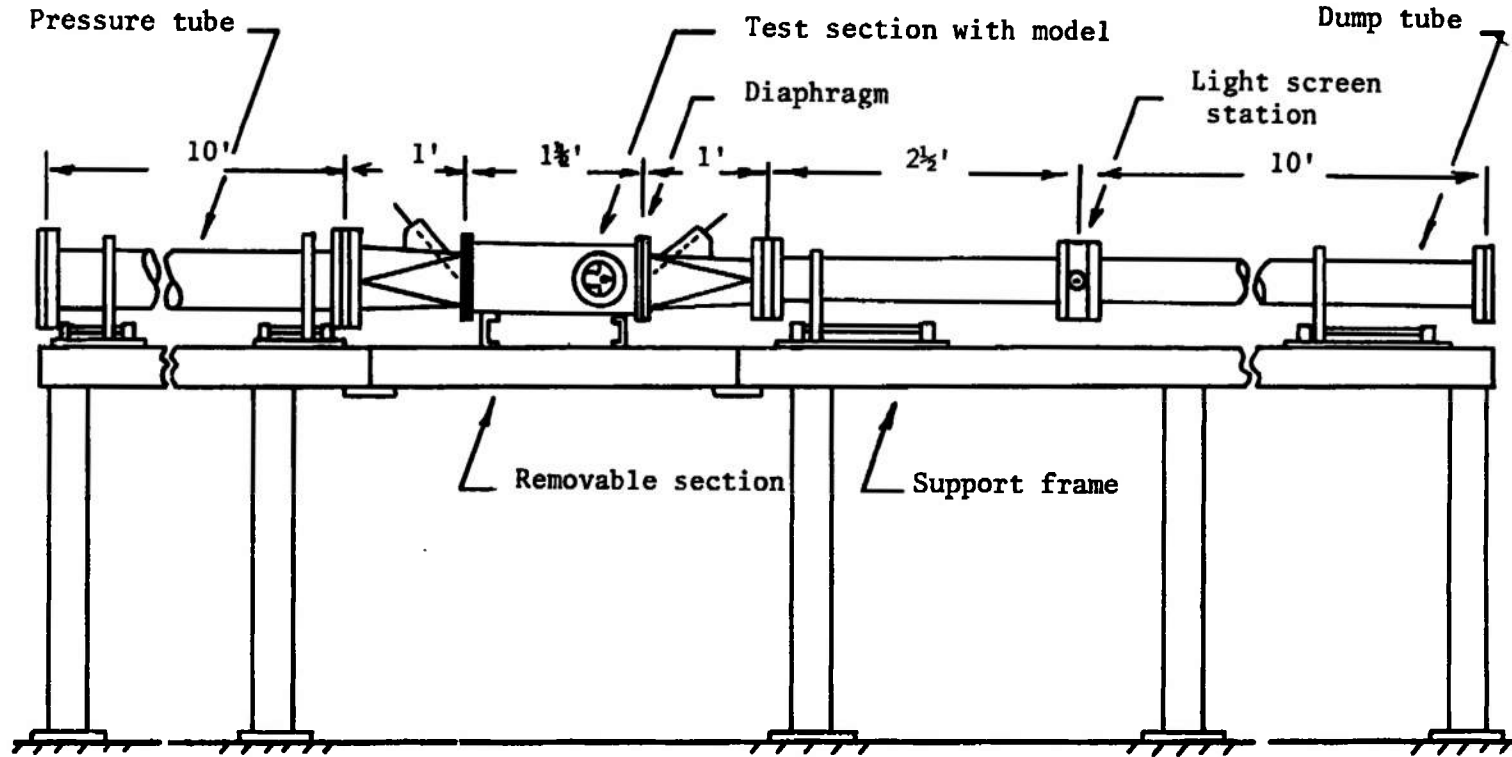
APPENDIX I

DETAILED DESCRIPTION OF LUDWIG TUBE WIND TUNNEL, NOZZLES,
AND AUXILIARY EQUIPMENT

A detailed side view of the tunnel is shown in Figure I.1. The overall length of the intermittent tunnel is 26 ft and it is fabricated entirely out of stainless steel 304. The high pressure end of the tunnel is made from a 10 ft. length of seamless tube with 5.295 in I.D. and 0.134 in. wall thickness. A transition piece made out of 1/8 in. plate and 1 ft in length connects the tube to a rectangular nozzle section 1 1/2 ft. in length and contains a diaphragm rupturing pin. The high pressure end of the tunnel and the transition piece are mounted on linear ball bushings which make it possible by a simple hand push to move the entire tube and transition piece 4 in. away from the nozzle section along the tunnel centerline. This permits insertion and removal of diaphragms for experiments with upstream diaphragm location. Screens may be introduced at this point. The nozzle section follows and will be described in greater detail below. For experiments with diaphragm downstream of nozzle and test section the diaphragm is placed between the nozzle section and another 1 ft transition section which contains the diaphragm rupturing pin and connects the nozzle section to the low pressure of dump tube. The dump tube is made of seamless tube 3.760 in. I.D. and 0.120 in. wall thickness and consists of two sections. The first section is 2 1/2 ft long and is connected to the transition piece. The other section is 10 ft in length. A 2 in. thick insert, the size of a 4 in. pipe flange, is located between these two pipes. The insert contains two quartz windows, 3/4 in. diameter and 1 in. thick, and permits a beam of light to pass through the tube. This arrangement acts as a shock detection station can be used to trigger the electronic instrumentation. The individual sections of the tube are sealed together by inserts containing O-rings placed between the flanges.

The downstream transition section and dump tube assembly are mounted on linear ball bushings which make it possible to move the entire assemble approximately 1 ft. away from the nozzle section along the tunnel centerline. This permits easy access to the test section as well as insertion and removal of diaphragms. The nozzle section, diaphragm and downstream transition section are held together by a wedge-shape clamping device. The clamping device permits quick connection and disconnection of the two parts of the tunnel.

The entire tunnel assembly is mounted on a 4in. I-beam and supported by several 4 in. diameter pipes. This arrangement is rigid and permits easy access to any part of the tube.



Pressure tube: 5.295 in. I.D., 0.134 in. wall, stainless steel 304 seamless tube.
 Dump tube: 3.760 in. I.D., 0.120 in. wall, stainless steel 304 seamless tube.
 Nozzle: two dimensional, 2 x 2 in. throat.

Figure I.1 Sketch of the intermittent tube wind tunnel

A 3 ft piece of the supporting I-beam for the test section is removable. The nozzle section and this portion of the I-beam may be lifted and the Mach-Zehnder interferometer (plate size; 4 1/8" x 7"), manufactured by Zeiss Company, positioned in place.

The nozzle section is rectangular with 2 in. by 5 in. inside dimensions and 1 1/2 ft in length. This section contains the nozzle blocks, test section and model support. The side walls extend to practically the entire length of the section and are sealed to it by means of O-rings. The nozzle blocks are 2 in. in width and rest on the top and bottom of the rectangular nozzle section. They are held in place by screws and are sealed by O-rings concentric with the screws. The side walls may be easily removed to exchange the nozzle blocks which have been machined out of Plexiglass. The windows are mounted and sealed in metal frames which in turn are sealed by means of O-rings into the side walls. Windows are held flush with the inside of the nozzle walls by threaded retaining rings. The windows are 4 in. diameter, 1 in. thick, and made of Schott BK-7 glass ground to 1/8 wave length with a wedge angle no greater than 20 min. The location of the windows is 5 in. upstream from the diaphragm. The model support is mounted in the nozzle section near the diaphragm. Models extend into the nozzle section, as viewed through the window, and are easily changed by reaching into the test section while the diaphragm is being changed. For a more detailed description of the equipment see reference 6.

Nozzles

The four nozzles that are used in the test section of the Yale Ludwig tube are listed as follows.

1. Y167 is a continuously expanding wedge type nozzle with an exit Mach number of 1.67. It has a three degree half angle diverging section and a six inch radius of curvature at the throat.
2. Y300 is a continuously expanding nozzle with an exit Mach number of 3.0. The contour of the supersonic section is a cubic curve.
3. Y160 is a parallel flow nozzle with a exit Mach number of 1.6. The contour of the supersonic section was calculated by the method of characteristics.
4. Y250 is a parallel flow nozzle with an exit Mach number of 2.5. The contour of the supersonic section was calculated by the method of characteristics.

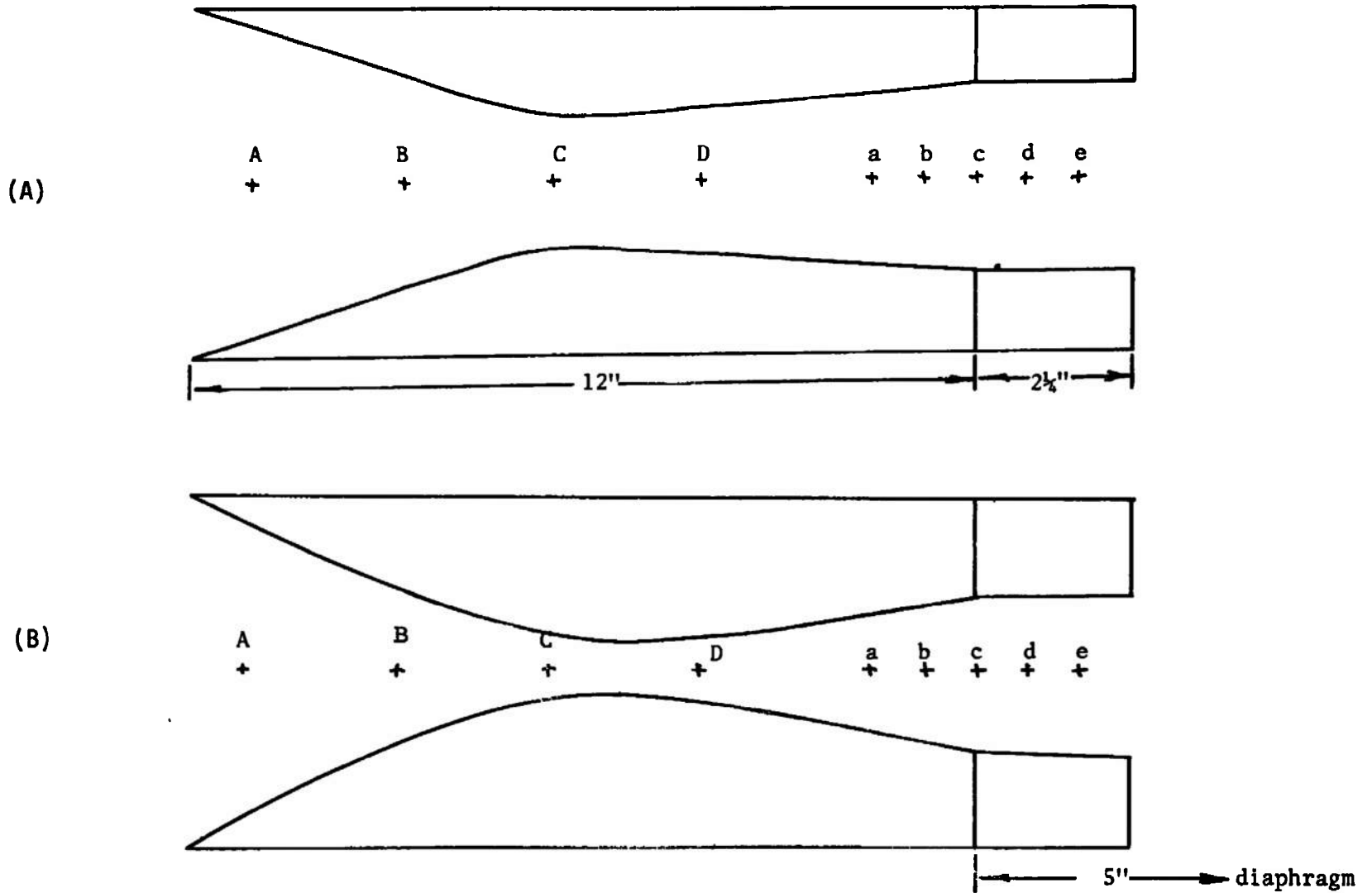


Figure 1.2. Nozzle profiles with extension blocks and pressure transducer locations, AB = BC = CD = 2.18", Da = 2.45", ab = bc = cd = de = 0.75".
 (A) Y167 Nozzle with 2.0" x 2.0" throat,
 (B) Y300 Nozzle with 2.0" x 0.58" throat.

Each nozzle has a set of extension blocks which are used to convert the nozzles from a semi-open jet to a closed jet configuration in the test section. A sketch of the Y167 and Y300 nozzles with extension blocks and the pressure transducer locations along the test section wall are shown in Figure I.2. The contour, throat radius of curvature and throat height of the Y160 and Y250 nozzles are shown in Figure I.3. Calibration curves for the Y160 and Y250 are shown in Figures I.4 and I.5 respectively. A sketch of the five degree half angle wedge model used in some of the experiments is shown in Figure I.6.

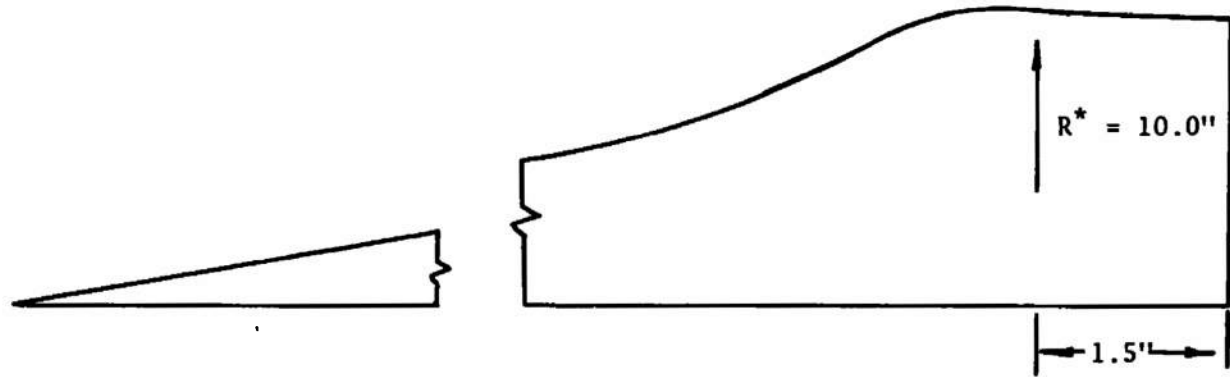
Instrumentation of the Tunnel

The tunnel is instrumented with a pressure measuring system, a photographic system, a Mach-Zehnder Interferometer, and a supporting electronic system. See Figure 2.

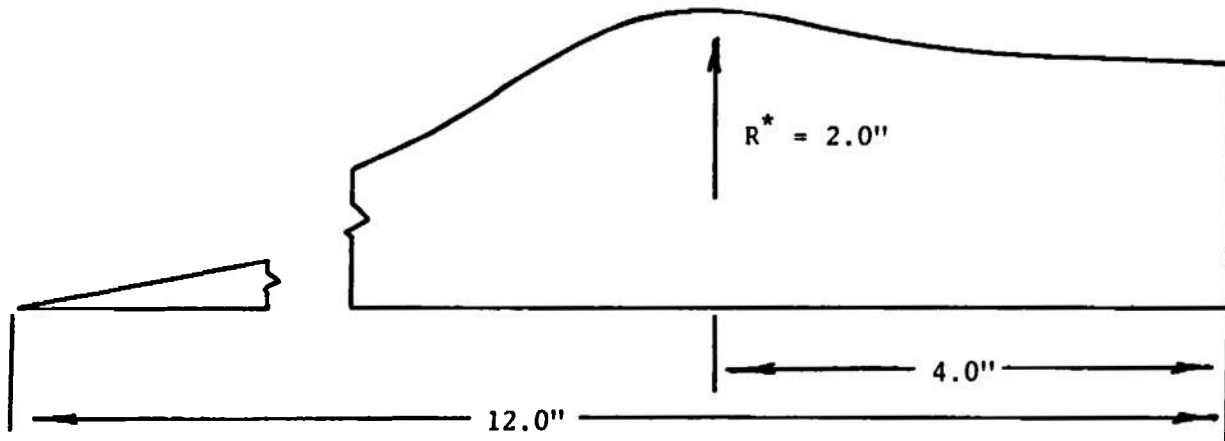
Transient pressure recordings are made with two piezo-electric quartz-crystal pressure transducers (Kistler Model 606L). The transducers may be mounted in an insert between the pressure tube and the upstream transition section, at the pressure tube end plate, and also in the nozzle side wall. The transducers can be mounted in a blank which replaces the window and/or along the side wall of the test section. They are mounted flush with the inside wall surface. The side wall locations are shown in Figure I.2. The output of the transducer is amplified by a Kistler Universal Dial-Gain Charge Amplifier Model 504 or 504A and it is recorded on an oscilloscope. The rise time is given to be 3 microseconds. Simultaneous pressure recordings at two different locations are obtained by using two pressure transducers and amplifiers.

The Mach-Zehnder Interferometer is located at the test section and is used for density measurements. This is done by streak and still interferograms. It may also be modified so that shadowgraph pictures can be taken. This is done by using the parallel light from the top light path and blocking the bottom light path at the compensating chamber. The same optics and light sources are used. Two light sources, a 100 watt continuous mercury arc lamp with a d.c. power supply and a spark source, can be mounted on the interferometer together with the appropriate lens systems. The continuous light source is used for streak interferograms and high-speed shadowgraph movies while the spark light source is used for still interferograms and shadowgraph pictures.

The flow field in the nozzle is recorded by shadowgraph methods in parallel light which is collimated by means of a f/6, 610 mm focal length Bausch & Lomb Aero Tessar aerial camera lens. A spark light source with a 0.08 cm diameter



(A)



(B)

Figure I.3. Nozzle profiles. (A) Y160 nozzle, (B) Y250 nozzle.
Each with a $2.0'' \times 0.5''$ throat.

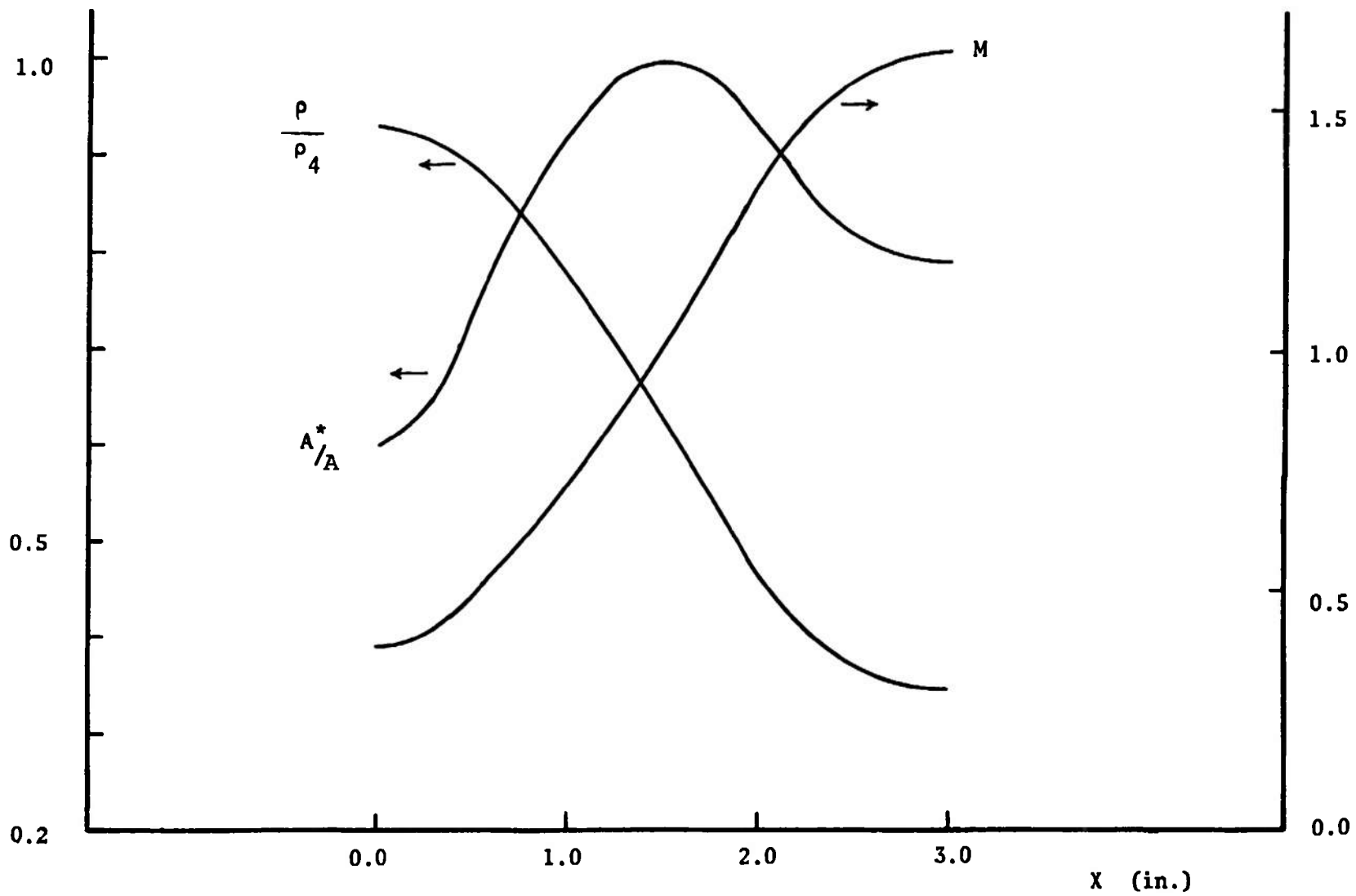


Figure I.4. Calibration curves for the Y160 nozzle.

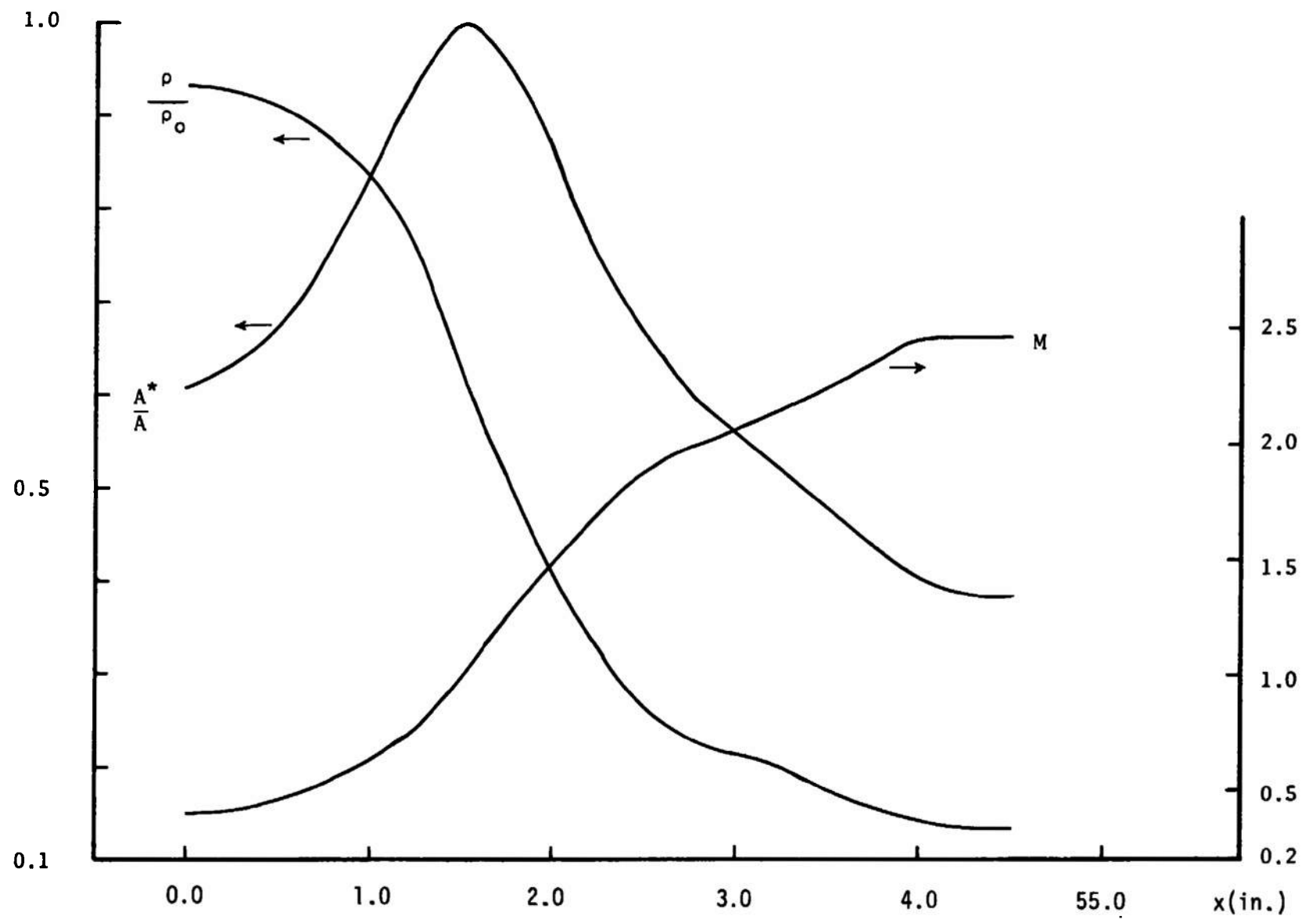


Figure I.5 Calibrations for the Y250 nozzle

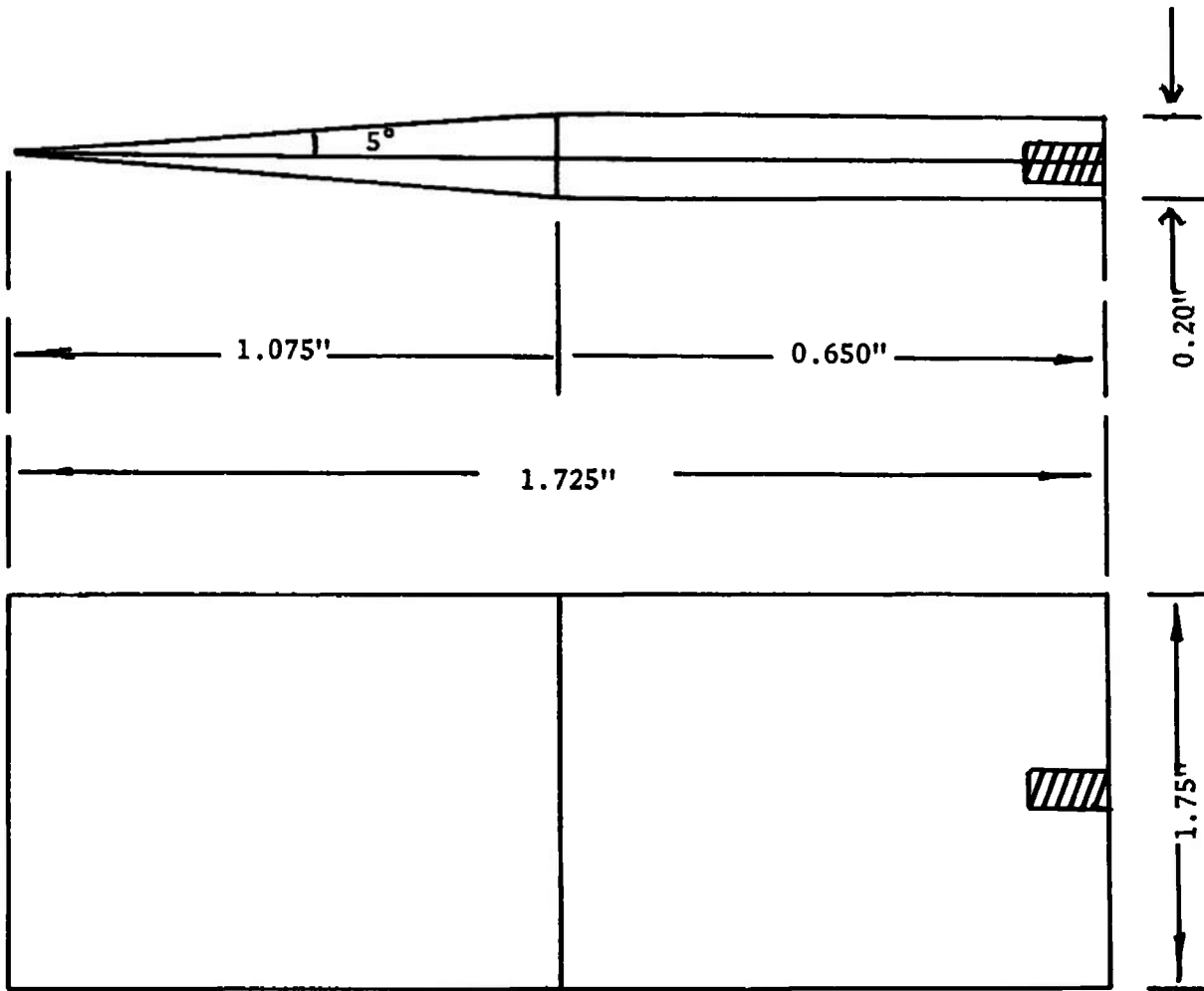


Figure I.6. Wedge model with dimensions

source is located at the focal point of the lens. The spark source unit has a duration of 0.5×10^{-6} sec. and is the type suggested by Kovaszney.* A detailed description of the spark source and its power supply used here may be found in Klikoff.**

The spark source may be triggered at any time after the shock wave generated by the ruptured diaphragm passes a position one inch downstream of the diaphragm. A pressure transducer (Kistler Model 606L) is located at this position. When the shock wave passes, the pressure transducer generates a signal which is amplified by a Kistler Universal Dial-Gain Charge Amplifier Model 504. This amplified signal is then fed into a time delay unit (General Radio Time Delay Generator, Type 1392-A) which in turn triggers a thyatron amplifier and spark source combination after any desired time interval.

Shadowgraphs are recorded on 4 x 5 in. type 52 Polaroid film, and the exposure is determined by the short duration (0.5×10^{-6} sec.) spark source. Shadowgraph movies of the flow in the nozzle are obtained by a Fastax 16 mm Model WF3 high-speed motion picture camera in the framing mode at approximately 5000 frames per second. Streak interferograms were made by using this camera in the streak mode (by removal of rotating prism). The light source in each case is a 100 watt mercury arc lamp driven by a 50 volt d.c. power supply.

* Kovaszney, L.S.G. 1949 High power short duration spark discharge. Rev. of Sci. Inst. 20, 696.

** Klikoff, W.A. 1965 Propagation of weak conical disturbances in relaxing supersonic flows. D. Eng. Thesis, Yale University, New Haven.

REFERENCES

1. Sedov, L. I., Similarity and Dimensional Methods in Mechanics, Academic Press, N. Y., 1959, Chapters 1 and 2.
2. Oswatitsch, K., "Similarity and Equivalence in Compressible Flow," Advances in Applied Mechanics, Ed. H. Dryden and Th. von Kármán, Vol 4, 1960, pp. 154-269.
3. Fila, L. J., "Preliminary Considerations in the Design of a Ludwieg Tube for High Reynolds Numbers," Arnold Engineering Development Center, Report No. AEDC-TR-67-210, February 1968.
4. Falk, T. J., "A Tube Wind Tunnel for High Reynolds Number Supersonic Testing," Office of Aerospace Research, U.S.A.F. Report No. ARL 68-0031, February 1968.
5. Ludwieg, H., "Der Rohrwindkanal," Zeitschrift für Flugwissenschaft, Jahrgang 3, Heft 7, July 1955, pp. 206-216; also Ludwieg, H., "Tube Wind Tunnel: A Special Type of Blow-down Tunnel," AGARD Rept. 143, July 1957, NATO Headquarters, Scheveningen, Holland.
6. Wegener, P. P. and Buzyna, G., "Experiments on Shock Stand-off Distance in Non-Equilibrium Flow," Journal of Fluid Mechanics, Vol. 37, Pt. 2, June 1969, pp. 325-335.
7. Cable, A. J. and Cox, R. N., "The Ludwieg Pressure-Tube Supersonic Wind Tunnel," The Aeronautical Quarterly, Vol. XIV, Pt. 2, May 1963, pp. 143-157.
8. Becker, E., "Grenzschichteffekte beim Rohrwindkanal," Jahrbuch der Wissenschaftliche Gesellschaft für Luftfahrt, Jan. 1957, WGL-Tagung Essen. Germany, pp. 232-237.
9. Shapiro, A. H., The Dynamics and Thermodynamics of Compressible Fluid Flow, The Ronald Press Company, N. Y. Vol I (1953) and Vol II (1954).
10. Bull, G. V., "Investigation into the Operating Cycle of a Two-Dimensional Supersonic Wind Tunnel," Journal of Aeronautical Sciences, Vol. 19, No. 9 September 1952, pp. 609-614.
11. Johnson, J. A., III and Cagliostro, D., "Experiments with a Supersonic Tube Wind-Tunnel," Arnold Engineering

Development Center, Final Report No. AEDC-TR-70-71, March 1970.

12. Johnson, J. A., III and Cagliostro, D., "Starting Phenomena in a Supersonic Tube Wind Tunnel," AIAA Journal, Vol. 9, No. 1, January 1971, pp. 101-105.
13. Johnson, J. A., III and Cagliostro, D., "Gasdynamic Starting Processes in a Supersonic Ludwieg Tube," Bulletin of the American Physical Society, Ser. II, Vol. 14, No. 4, April 1969, p. 527.
14. Cagliostro, D.J., "Starting Processes in a Supersonic Ludwieg Tube", Bulletin of the American Physical Society, Ser. II, Vol. 16, No. 11, November 1971, p. 1308.
15. Dayman, B., Jr., "Blocking in the Supersonic Wind Tunnel," Journal of the Aeronautical Sciences, Vol. 25, No. 4, April 1958, pp. 264-265.

DOCUMENT CONTROL DATA - R & D

(Security classification of title, body of abstract and indexing annotation must be entered when the overall report is classified)

1. ORIGINATING ACTIVITY (Corporate author) Yale University New Haven, Connecticut		2a. REPORT SECURITY CLASSIFICATION UNCLASSIFIED	
		2b. GROUP N/A	
3. REPORT TITLE EXPERIMENTS ON THE STARTING PROCESS IN A LUDWIG TUBE			
4. DESCRIPTIVE NOTES (Type of report and inclusive dates) Interim Report - June 1970 to January 1972			
5. AUTHOR(S) (First name, middle initial, last name) Dominic J. Cagliostro			
6. REPORT DATE March 1972	7a. TOTAL NO OF PAGES 51	7b. NO. OF REFS 15	
8a. CONTRACT OR GRANT NO. F40600-70-C-0008	8a. ORIGINATOR'S REPORT NUMBER(S) AEDC-TR-72-42		
b. PROJECT NO	8b. OTHER REPORT NO(S) (Any other numbers that may be assigned this report) N/A		
c. Program Element 65802F			
d.			
10. DISTRIBUTION STATEMENT Approved for public release; distribution unlimited.			
11. SUPPLEMENTARY NOTES Available in DDC		12. SPONSORING MILITARY ACTIVITY Arnold Engineering Development Center (XON), Air Force Systems Command, Arnold AF Station, Tenn. 37389	
13. ABSTRACT An experimental investigation of the starting process in the Ludwig tube, an intermittent type tube wind-tunnel, was conducted with emphasis on the effects of nozzle-test section geometry. In particular the semi-open and closed jet configuration was studied. Dry air at 1.0 and 2.0 atm pressure and room temperature was used in the supply tube and a quick opening diaphragm located downstream of the nozzle and test section was employed to initiate the flow. Spark shadowgraph pictures, high-speed shadowgraph movies, streak interferograms, and pressure measurements were made in $M = 1.67$ and 3.0 continuously expanding nozzles and $M = 1.6$ and 2.5 parallel flow nozzles. Results show that the nozzle-test section geometry significantly affects the starting process in the $M = 1.60$ and 1.67 nozzles. In the semi-open jet configuration supersonic flow was established without the formation of starting shocks, while in the closed jet configuration a starting shock wave did occur. Boundary layer thickening and flow separation occurred during the starting process in the $M = 2.50$ and 3.0 nozzles. Adverse pressure and density gradients were measured in the nozzle during the starting process. This effect appears to cause the observed boundary layer thickening and flow separation which occur during that period in the $M = 2.5$ and 3.0 nozzles. These results indicate that viscous effects are important during the starting process in a Ludwig tube under the conditions tested here. It was found that the presence of a model in the $M = 1.67$ nozzle in a closed jet configuration increased the starting times.			

14. KEY WORDS	LINK A		LINK B		LINK C	
	ROLE	WT	ROLE	WT	ROLE	WT
hypervelocity wind tunnels shock tubes wind tunnel nozzles high speed photography boundary layer separation						

AFPC
Aresid A79 Team